



---

## *Robotics 2*

# Human-Robot Coexistence and Collaboration

Prof. Alessandro De Luca

DIPARTIMENTO DI INGEGNERIA INFORMATICA  
AUTOMATICA E GESTIONALE ANTONIO RUBERTI





# Human-friendly robotics

The goal



traditional  
robotics



replacing  
humans



human-  
friendly  
robotics



collaborating  
with humans



co-workers on factory floor



personal robots in service



# SAPHARI concept

Place the human at the center of the entire robot development



FP7 ICT  
EU project  
(2011-15)

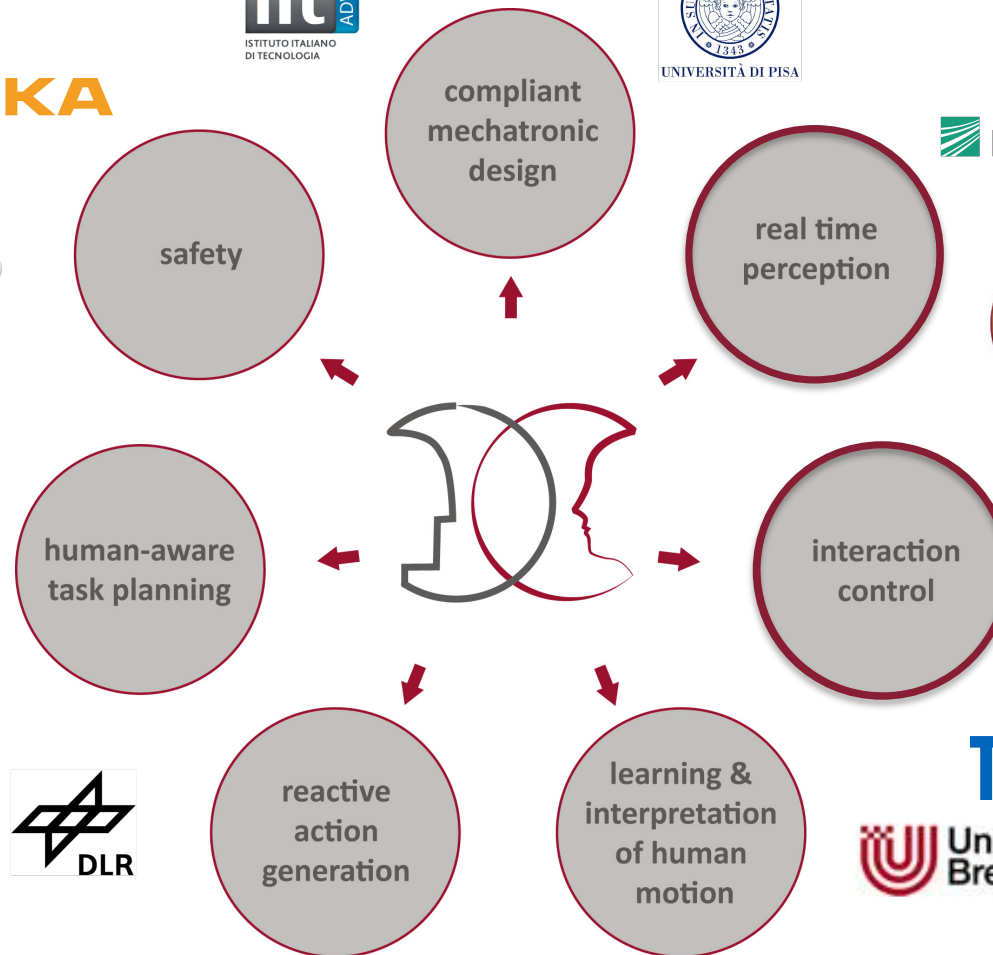
KUKA

EADS

LAAS-CNRS



SAPIENZA  
UNIVERSITÀ DI ROMA  
(coordinator)



address all essential aspects of safe and intuitive **physical interaction**  
between humans and complex human-like robots in a strongly integrated way



# Handling of collisions and intentional contacts

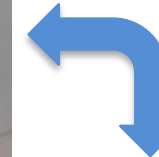
Basic **safety-related control** problems in physical Human-Robot Interaction (**pHRI**)



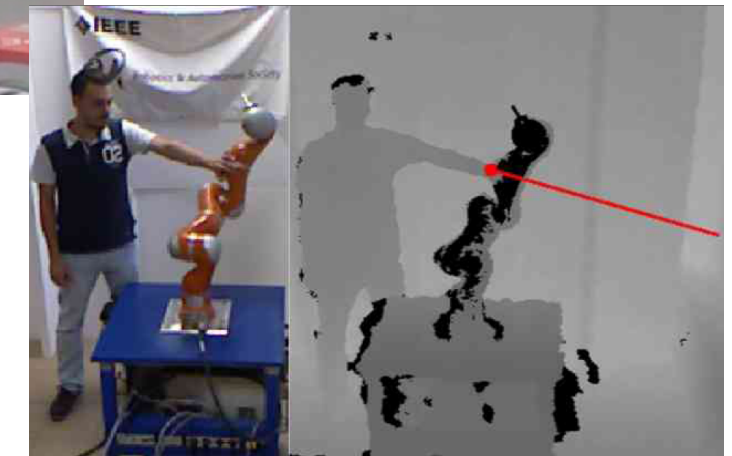
collision **detection/isolation** and **reaction**  
**(without** the use of external sensing)



workspace monitoring  
for **continuous**  
**collision avoidance**  
(while the task is running)



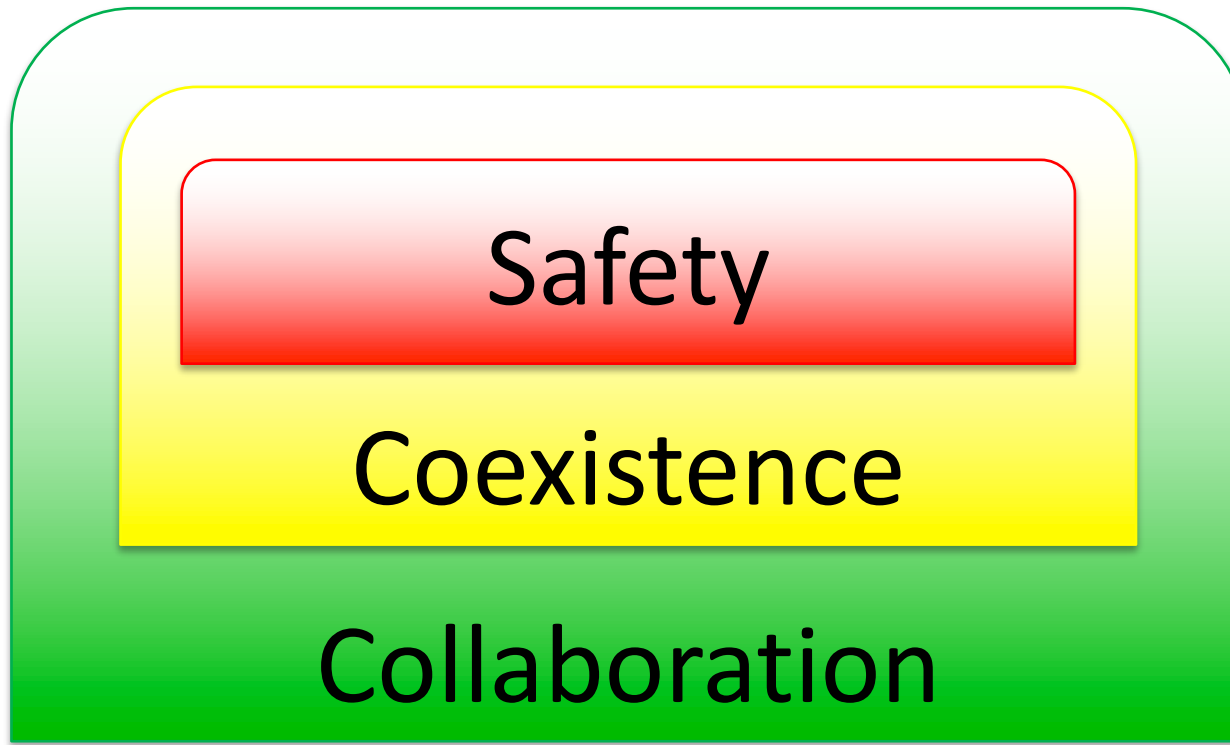
estimation and control  
of **intentional forces**  
exchanged at the contact  
**(with or without a F/T sensor)**  
for human-robot collaboration





# Safe physical Human-Robot Interaction (pHRI)

Control architecture of consistent robot behaviors (De Luca, Flacco: IEEE BioRob 2012)



- **integrated design & use** of soft mechanics, actuation, (proprio- and exteroceptive) sensing, communication, and **control** algorithms



# Physical HRI

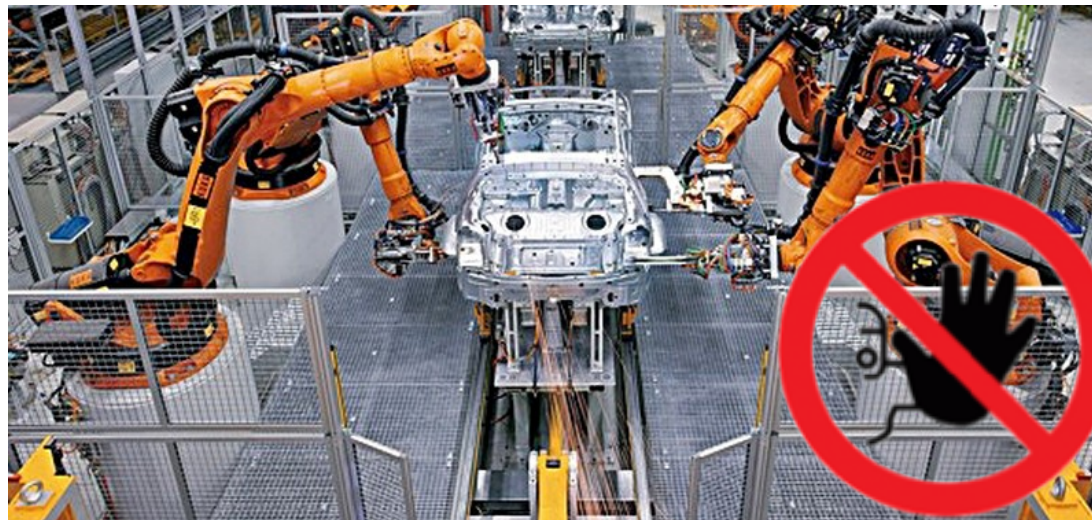
Hierarchy of consistent behaviors

## Safety

lightweight mechanical design  
compliance at robot joints

**Safety** is the most important feature of a robot that has to work close to human beings

Classical solutions for preserving safety in industrial environments, i.e., using cages or stopping the robot in the presence of humans [**ISO 10218**], are inappropriate for pHRI





# Physical HRI

Hierarchy of consistent behaviors



**Coexistence** is the robot capability of sharing the workspace with other entities, most relevant with humans

Human (and robot!) safety requirements must be always guaranteed (i.e., **safe coexistence**)



original robot task

sharing the workspace  
without the need of physical contacts

safe HR coexistence



# Physical HRI

Hierarchy of consistent behaviors

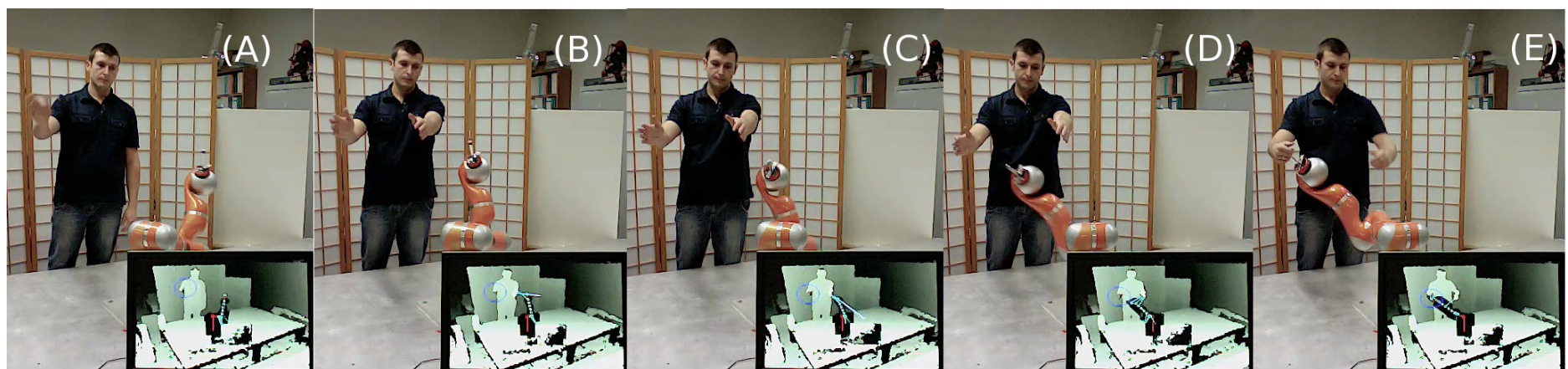


**Collaboration** occurs when the robot performs complex tasks with direct human interaction and coordination

Two modalities which are not mutually exclusive:  
**contactless** and **physical**

gestures or voice commands  
visual coordination

with intentional contact  
and exchange of forces

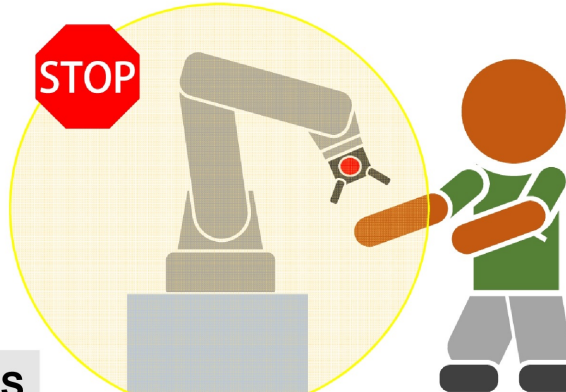




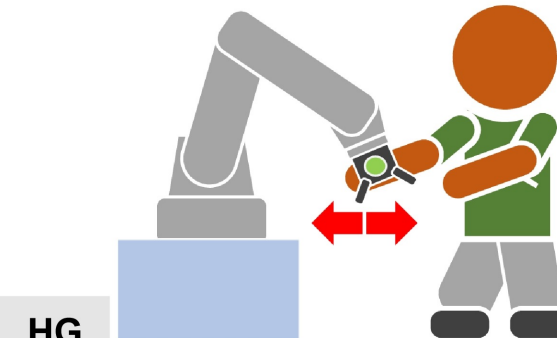
# Types of collaborative operations

From ISO 10218-1:2011 & 10218-2:2011 standards (refined in ISO-TS 15066:2016)

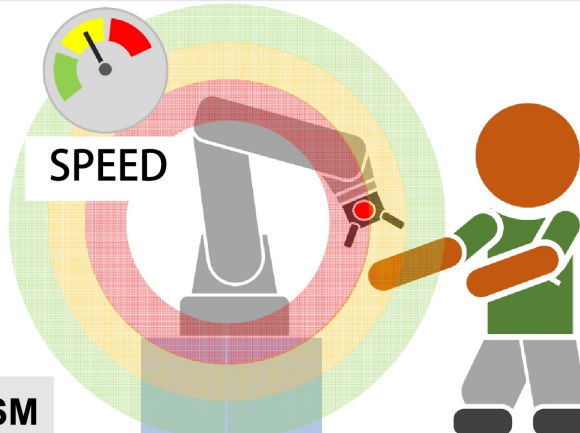
**LEVEL 1 - Safety-rated monitored stop**



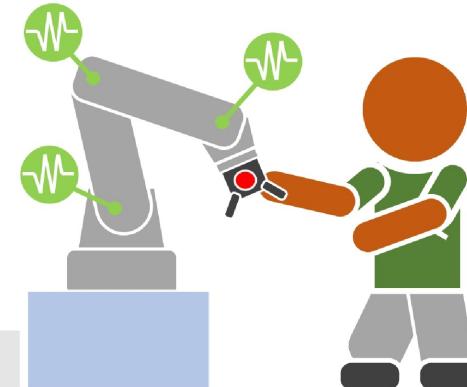
**LEVEL 2 - Hand guiding**



**LEVEL 3 - Speed and separation monitoring**



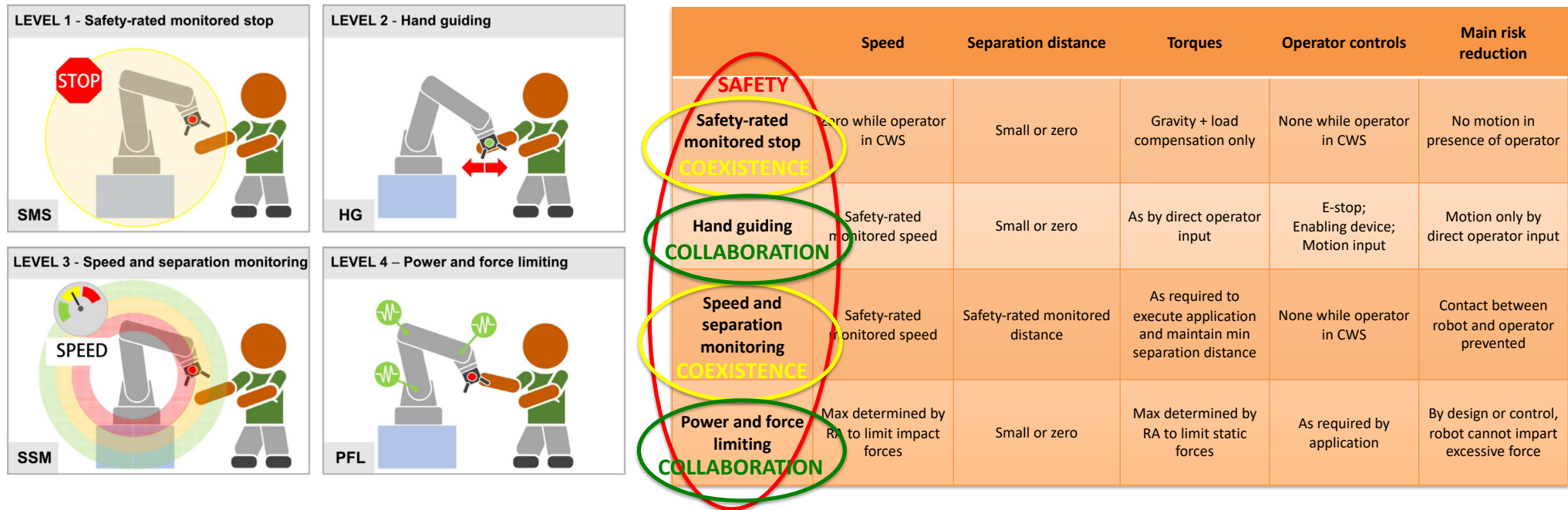
**LEVEL 4 – Power and force limiting**



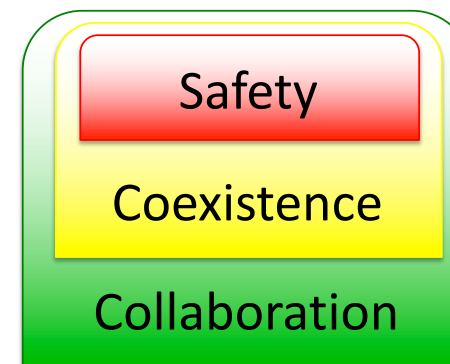
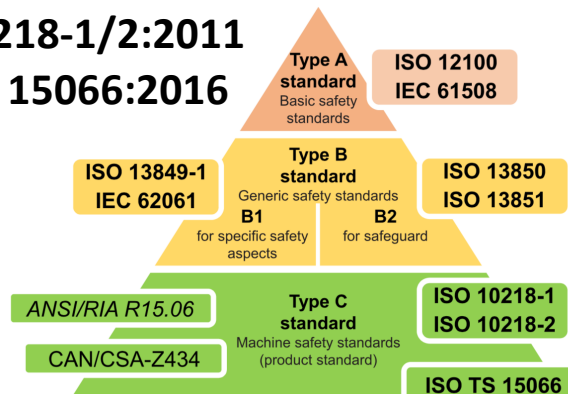


# Qualification of our control architecture for pHRI

## Relation with ISO Standard 10218 and Technical Specification 15066



**ISO 10218-1/2:2011**  
**ISO/TS 15066:2016**

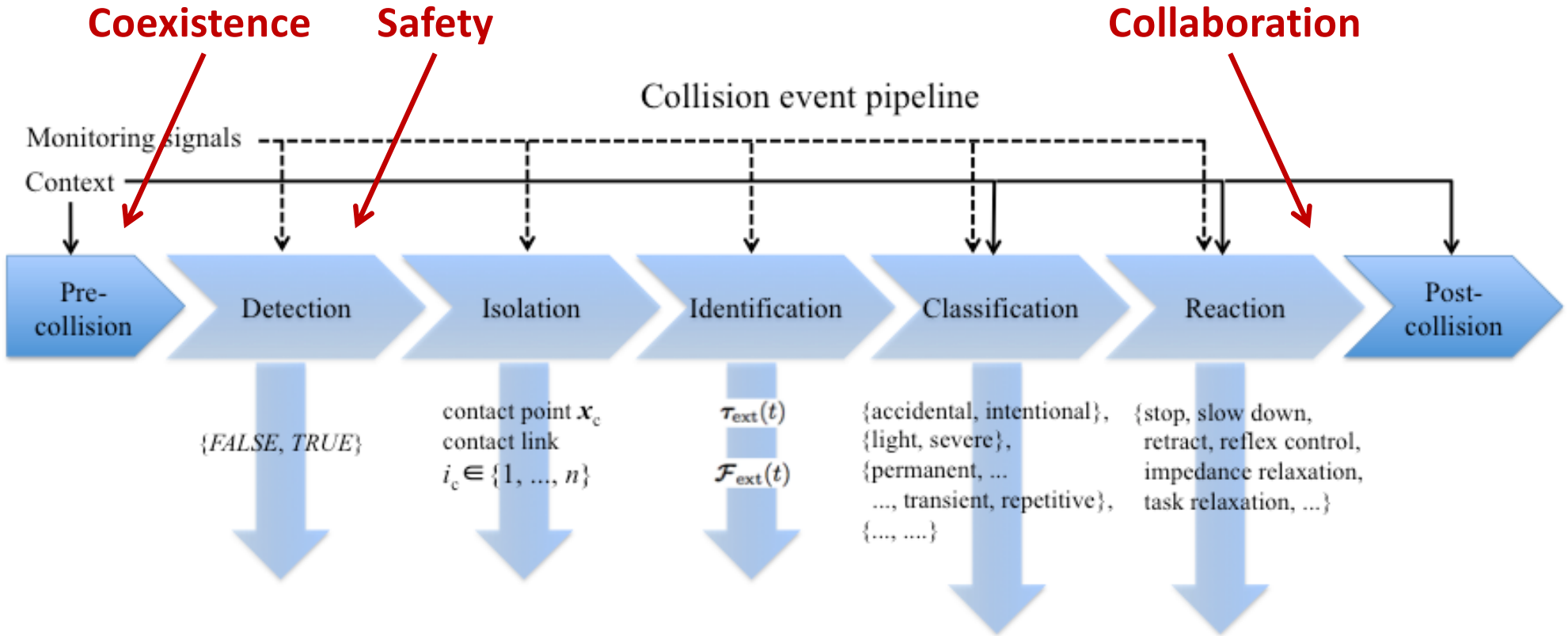


- collision detection and reaction
- workspace sharing
  - with collision avoidance
- coordinated motions & actions
  - with/without contact



# Control levels in the collision event pipeline

Haddadin, De Luca, Albu-Schäffer: IEEE T-RO 2017



**Monitoring signals** can be generated from sensors or models (signal- or model-based methods)

**Context** information is needed (or useful) to take the right or most suitable decisions



# Collision detection and reaction

Residual-based experiments on DLR LWR-III (IROS 2006, IROS 2008)



- collision detection followed by different **reaction** strategies
- **zero-gravity** behavior: gravity is always compensated first (by control)
- detection time: 2-3 ms, reaction time: + 1 ms

3 videos

		
admittance mode	reflex torque	reflex torque
first impact at 60°/s		first impact at 90°/s
$\dot{q}_r = K_Q r$		$\tau = K_R r$



# Coexistence

Early days and yesterday ...



video

informational video by National Institute  
for Occupational Safety and Health (USA)



video

commercial video by ABB Robotics  
on EPS (Electronic Position Switch)  
and early SafeMove software



# Coexistence

Today and tomorrow? ...

## SafeMove2

Safety certified monitoring of robot motion,  
tool and standstill supervision

Nov 2016, Singapore

2016

IROS 2013  
Best Video Award Finalist



(using 1 Kinect  
depth sensor)

video

video

commercial video by ABB Robotics  
of SafeMove2 software  
(using 2 laser scanners)

<https://youtu.be/pIIhY8E3HFg>



## Safe Physical Human-Robot Collaboration

Fabrizio Flacco Alessandro De Luca

Robotics Lab, DIAG  
Sapienza Università di Roma

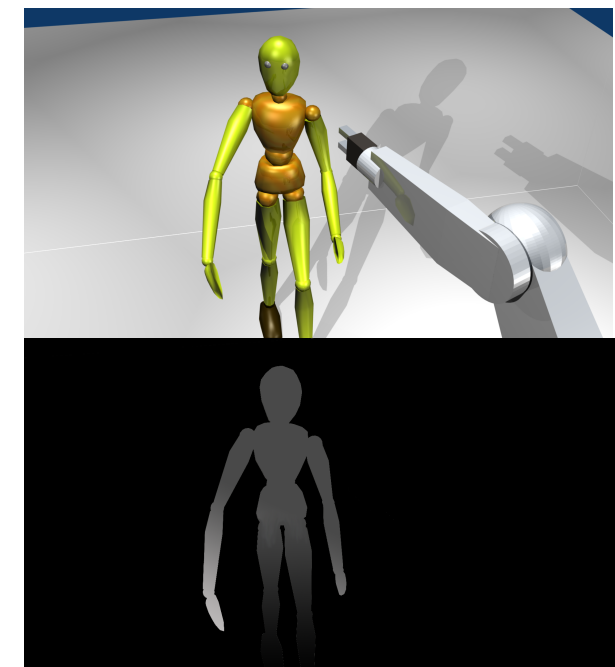
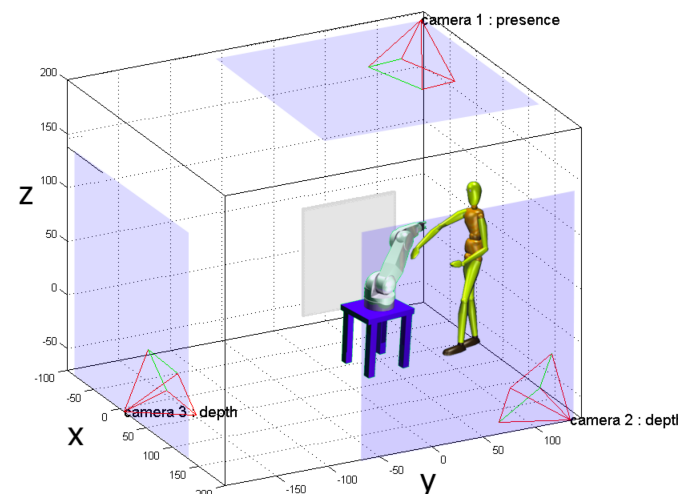
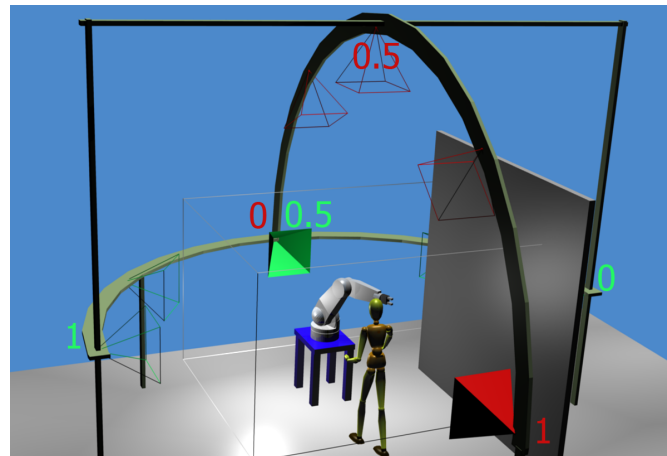
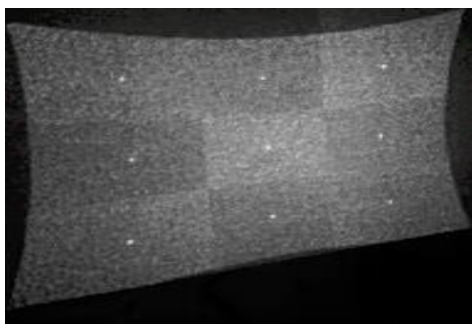
March 2013



# Collision avoidance

Using exteroceptive sensors to monitor robot workspace (ICRA 2010)

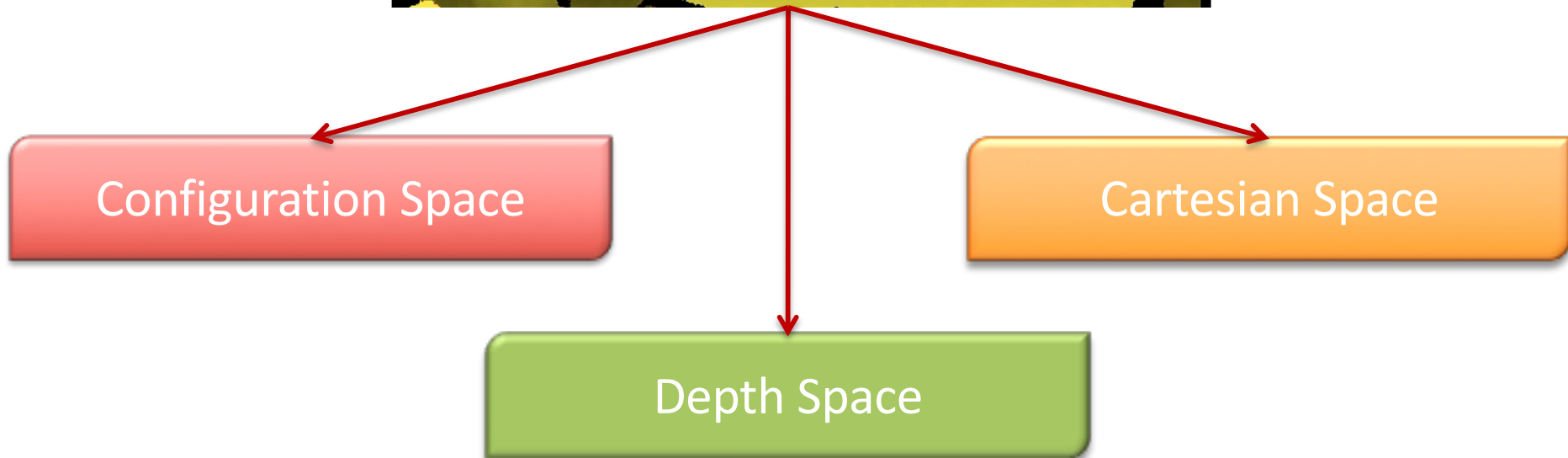
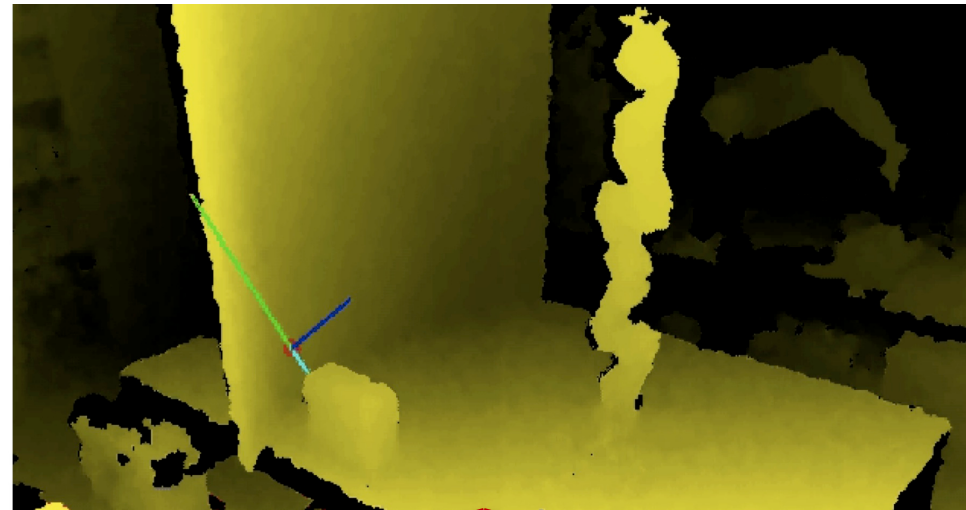
- **external sensing:** stereo-camera, TOF, structured light, depth, laser, presence, ... placed optimally to minimize occlusions (robot can be removed from images)





# Depth image

How to use it?





## Cartesian space

A long process

# Fusing multiple Kinects to survey human-robot workspaces

C. Lenz, M. Grimm, T. Röder, A. Knoll

Robotics and Embedded Systems  
Technische Universität München

video

TU Munich



# Configuration space

Possible, but typically only for few dofs

Real time control for safe human-robot coexistence using stereo vision

The manipulator performs the assigned task until an unknown obstacle is detected.

video

Univ Pisa



# Depth space

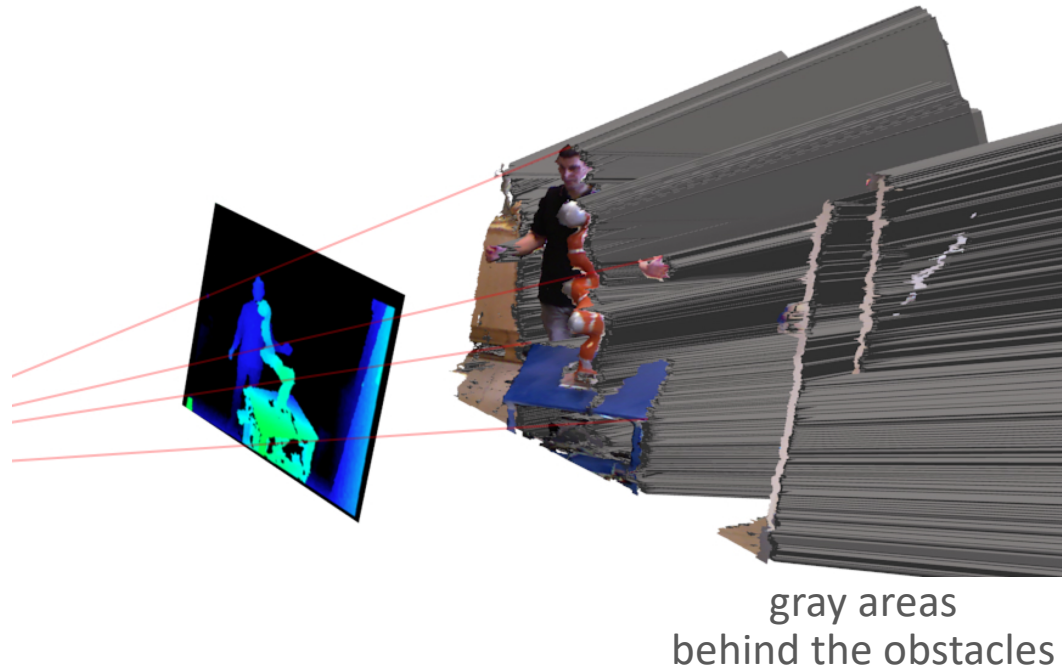
A 2.5-dimensional space

- non-homogeneous 2.5 dimensional space
  - $x, y$  position of the point in the image plane [pixel]
  - $d$  depth of the point with respect to the image plane [m]
- depth space is modeled as a pin-hole sensor
- point in Cartesian reference frame  $\mathbf{P}_R = (x_R, y_R, z_R)$
- point in sensor frame  $\mathbf{P}_C = \mathbf{R}\mathbf{P}_R + \mathbf{t} = (x_C, y_C, z_C)$
- point in depth space

$$p_x = \frac{x_C f s_x}{z_C} + c_x$$

$$p_y = \frac{y_C f s_y}{z_C} + c_y$$

$$d_p = z_C$$





# Depth space

## Distance evaluation

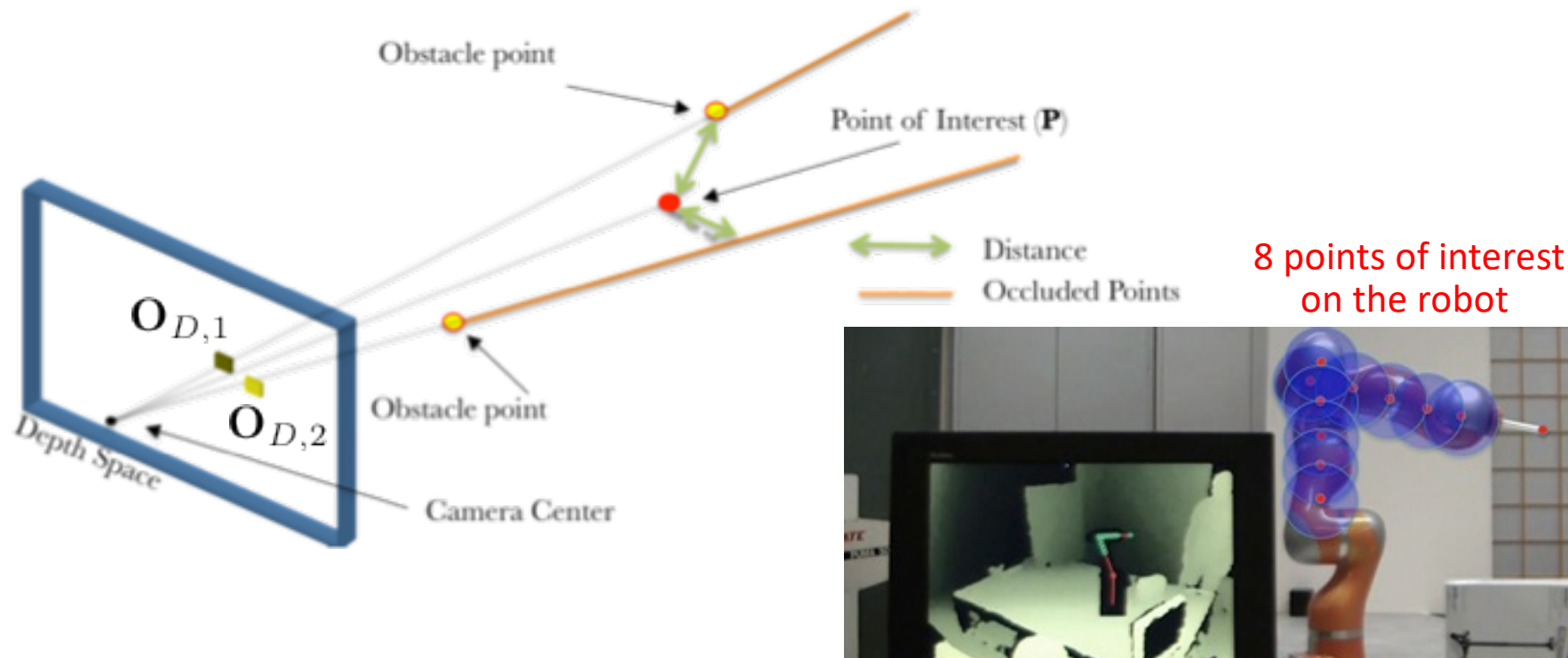
- distance between a **point of interest**  $\mathbf{P}_D = (p_x, p_y, d_p)$  and an **obstacle point**  $\mathbf{O}_D = (o_x, o_y, d_o)$

$$\text{dist}(\mathbf{P}, \mathbf{O}) = \sqrt{v_x^2 + v_y^2 + v_z^2}$$

$$v_x = \frac{(o_x - c_x)d_o - (p_x - c_x)d_p}{fs_x} \quad v_y = \frac{(o_y - c_y)d_o - (p_y - c_y)d_p}{fs_y} \quad v_z = d_o - d_p$$



(if obstacle point is closer than point of interest, set  $d_o = d_p$ )





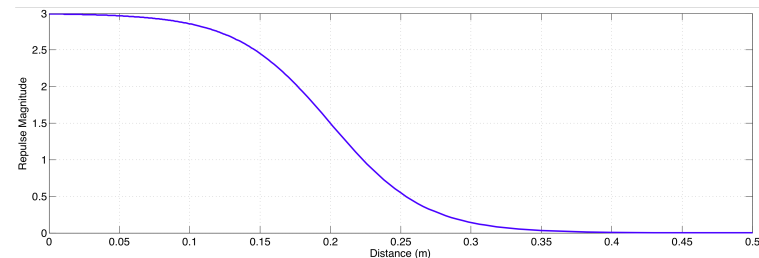
# Repulsive vector

A version of artificial potentials

- repulsive vector generated from the distance vector  $\mathbf{D}(\mathbf{P}, \mathbf{O}) = (v_x, v_y, v_z)$

$$\mathbf{V}_C(\mathbf{P}, \mathbf{O}) = v(\mathbf{P}, \mathbf{O}) \frac{\mathbf{D}(\mathbf{P}, \mathbf{O})}{\|\mathbf{D}(\mathbf{P}, \mathbf{O})\|}$$

$$v(\mathbf{P}, \mathbf{O}) = \frac{V_{max}}{1 + e^{\|\mathbf{D}(\mathbf{P}, \mathbf{O})\|(2/\rho)\alpha - \alpha}}$$



- repulsive vectors due to all obstacles near to point of interest are considered
  - orientation  $\Rightarrow$  sum of all repulsive vectors, magnitude  $\Rightarrow$  nearest obstacle only
  - inclusion of a pivoting strategy to avoid local minima or “too fast” obstacles

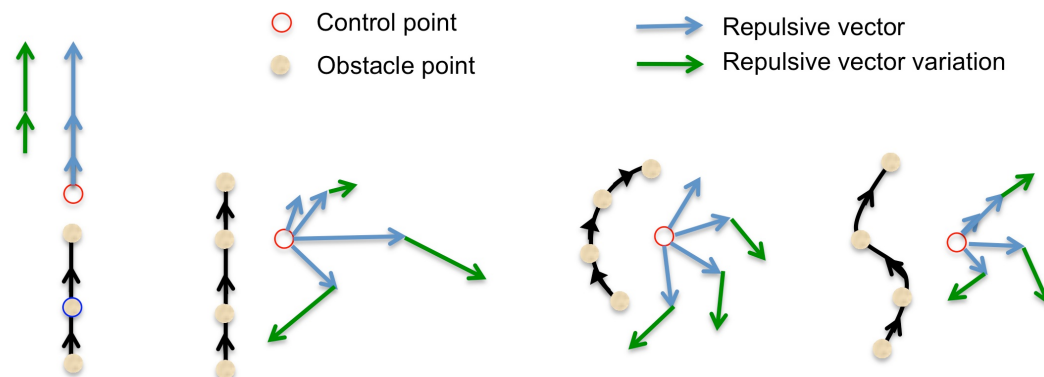
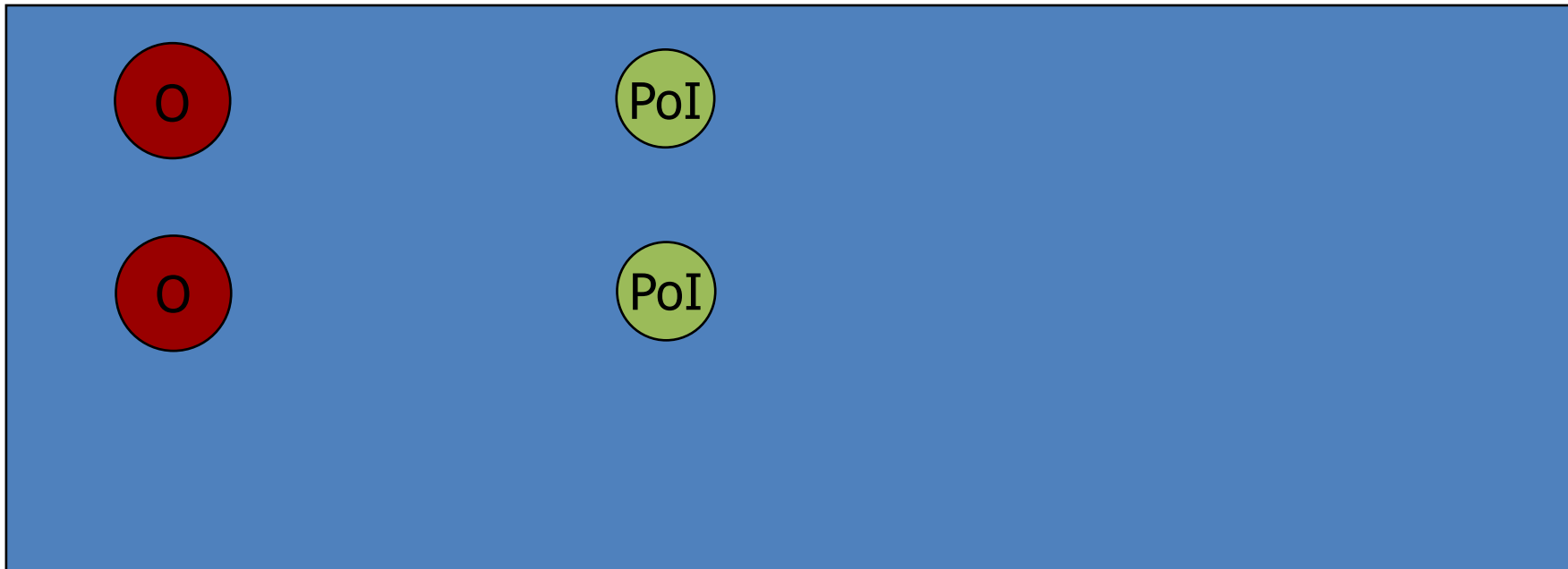




# Obstacle velocity

The pivot method (similar to a vortex field)

- for moving obstacles that are faster than the control point (on the robot)



○ Control point  
● Obstacle point

→ Repulsive vector  
→ Repulsive vector variation

$$\mathbf{a} = \frac{\dot{\mathbf{V}}_R(\mathbf{P})}{\|\dot{\mathbf{V}}_R(\mathbf{P})\|}, \quad \mathbf{r} = \frac{\mathbf{V}_R(\mathbf{P})}{\|\mathbf{V}_R(\mathbf{P})\|}, \quad \beta = \arccos(\mathbf{a}^T \mathbf{r})$$

if  $\beta < \frac{\pi}{2}$  then

$$\mathbf{n} = \mathbf{a} \times \mathbf{r}, \quad \mathbf{v} = \frac{\mathbf{n} \times \mathbf{a}}{\|\mathbf{n} \times \mathbf{a}\|},$$

$$\gamma = \beta + \frac{\beta - \frac{\pi}{2}}{1 + e^{-(\|\mathbf{V}_R(\mathbf{P})\|(2/\dot{\mathbf{V}}_{R_{max}}) - 1)}},$$

$$\mathbf{V}_{R_{pivot}}(\mathbf{P}) = \|\mathbf{V}_R(\mathbf{P})\| (\cos \gamma \mathbf{a} + \sin \gamma \mathbf{v})$$

else

$$\mathbf{V}_{R_{pivot}}(\mathbf{P}) = \mathbf{V}_R(\mathbf{P})$$

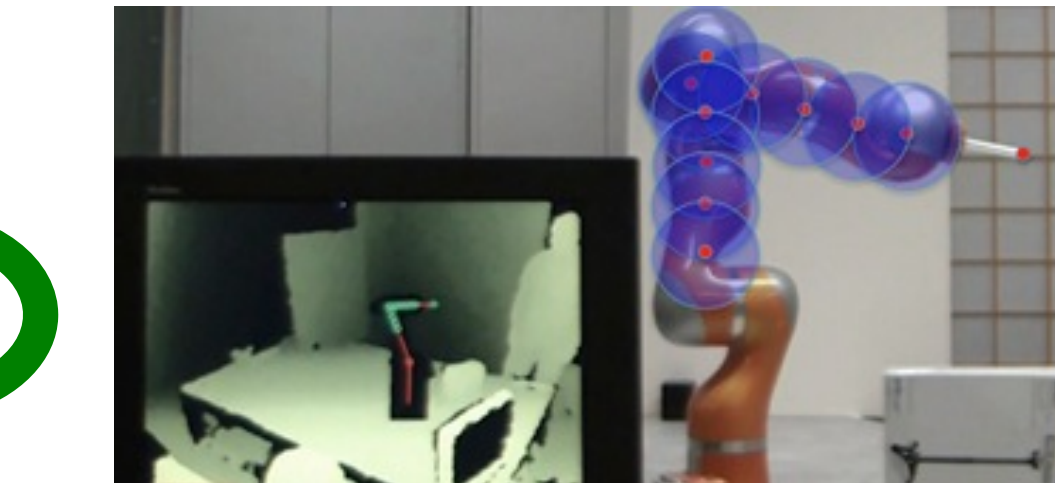
end if



# Motion control

Different handling of end-effector and other control points on the robot

- end-effector repulsive vector → repulsive velocity added to the original task velocity
- collision avoidance for the whole robot body (e.g., 8 control points)
  - repulsive vector
  - Cartesian constraints
  - joint velocity limits modification (using SNS)
- fluid, jerk-limited motion → human feeling of safety



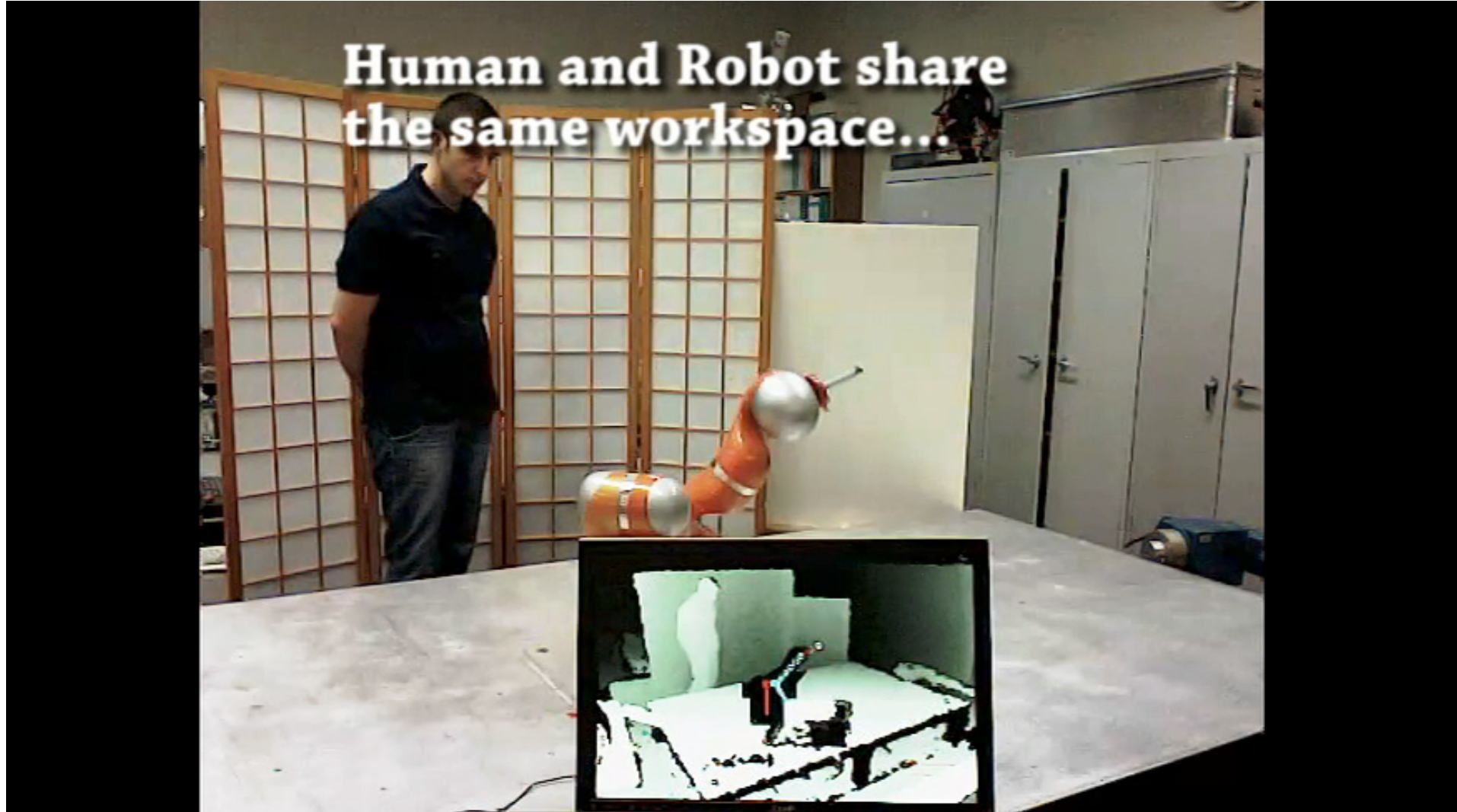
**Reflexxes**  
GmbH

[www.reflexxes.com](http://www.reflexxes.com)



# Safe coexistence

Collision avoidance in depth space (BioRob 2012)



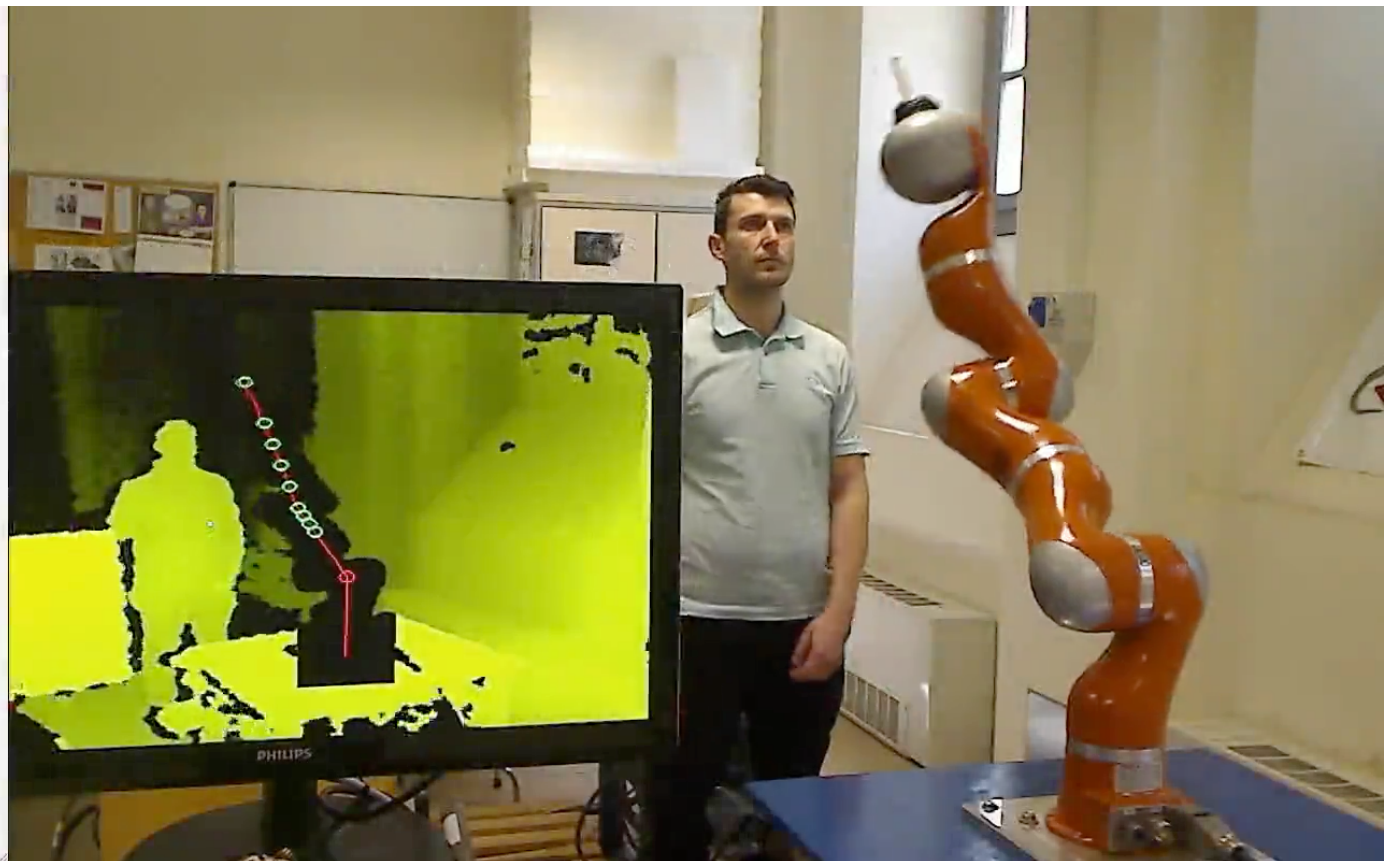
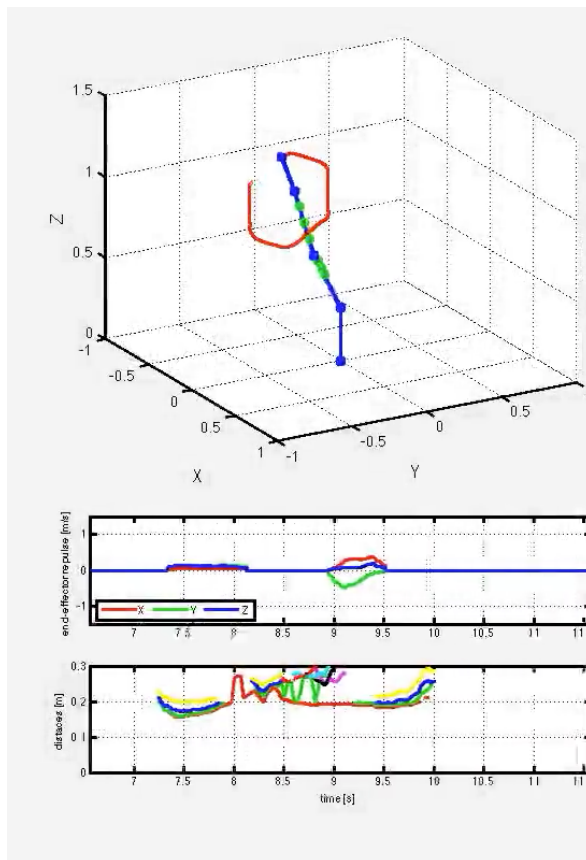
video



# Safe coexistence

Collision avoidance in depth space (ICRA 2012, J. Intell. & Rob. Syst. 2015)

video



resuming a cyclic Cartesian task as soon as possible ...



# Monitoring the workspace with two Kinects

... without giving away the depth space computational approach (RA-L 2016)

When a single camera is used the robot avoids occluded points even when generated by a far obstacle; the second camera will avoid this



# video

[https://youtu.be/WIw\\_Uj\\_ooYI](https://youtu.be/WIw_Uj_ooYI)

## real-time efficiency

algorithm extremely fast also  
with 2 devices: **300 Hz** rate  
(RGB-D camera has 30 fps)

### **problems solved by the second camera**

- + eliminates collision with false, far away “shadow” obstacles
  - + reduces to a minimum gray areas, thus detects what is “behind” the robot
  - + relative calibration of the two Kinects is done off-line



# SYMPLEXITY cell for robotized work on metallic surfaces

For abrasive finishing/fluid jet polishing tasks & for **human-robot quality assessment**

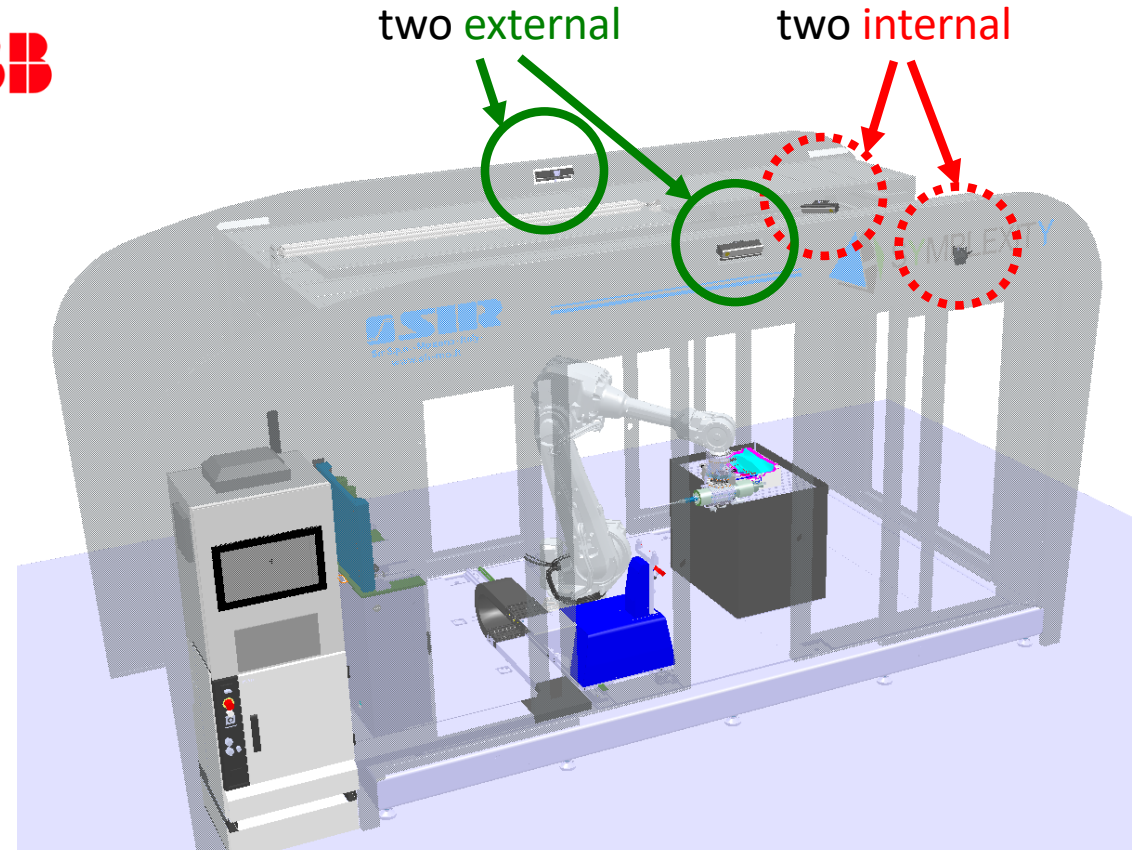


SYMPLEXITY

H2020 FoF EU project (2015-18)

ABB

- ABB IRB 4600-60 robot, with integrated SafeMove option
- certified communication with cell PLC, using ProfiSAFE protocol
- due to the intrinsic risks in the technological process, only for **HR coexistence** during visual check and measuring phase or for **contactless collaboration**
- **2 external** Kinects to recognize human gestures (e.g., automatic door opening, ...)
- initially ... **2 internal** Kinects (placed at the top corners of the cabin) for monitoring human-robot distances



**SIR**  
ROBOTIC SOLUTIONS

CLEMENTIANI STUDIORVM MUNINENSER ET REGGIOENSIS  
1751

**UNIMORE**  
UNIVERSITÀ DEGLI STUDI DI  
MODENA E REGGIO EMILIA

**SAPIENZA**  
UNIVERSITÀ DI ROMA



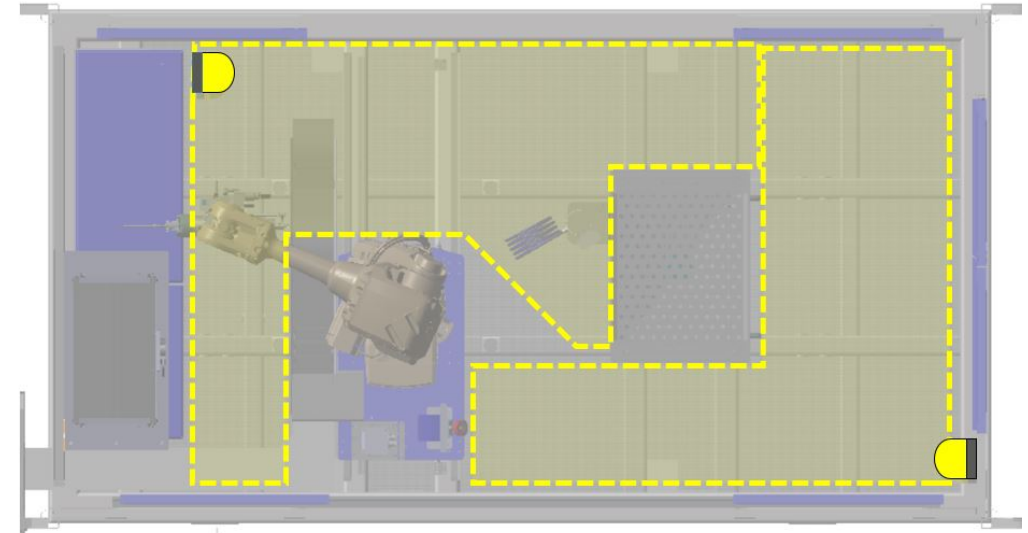
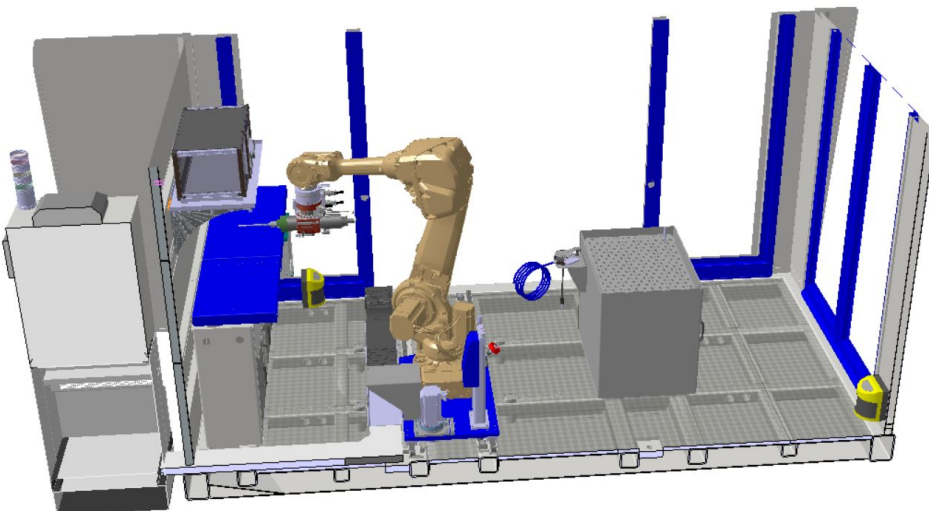
# Additional safety hardware

Certified laser scanners to be used in parallel with the Kinects



SYMPLEXITY

H2020 FoF EU project (2015-18)



- **two laser scanners** KEYENCE SZ-V 32n placed at calf height ( $\sim 50$  cm)
- maximize **coverage** of the free area inside the cell
- each sensor localizes the (radial) position of the operator in the cell, estimating an **approximate/conservative distance** to the robot
- **no missed situations**: robot slows down or stops according to sensed distance/area
- a **cascaded solution** of Kinects/laser scanners is a viable compromise between **certified safety** and more flexible sharing of the 3D workspace by human and robot



# CAD robot model and equipment in depth images

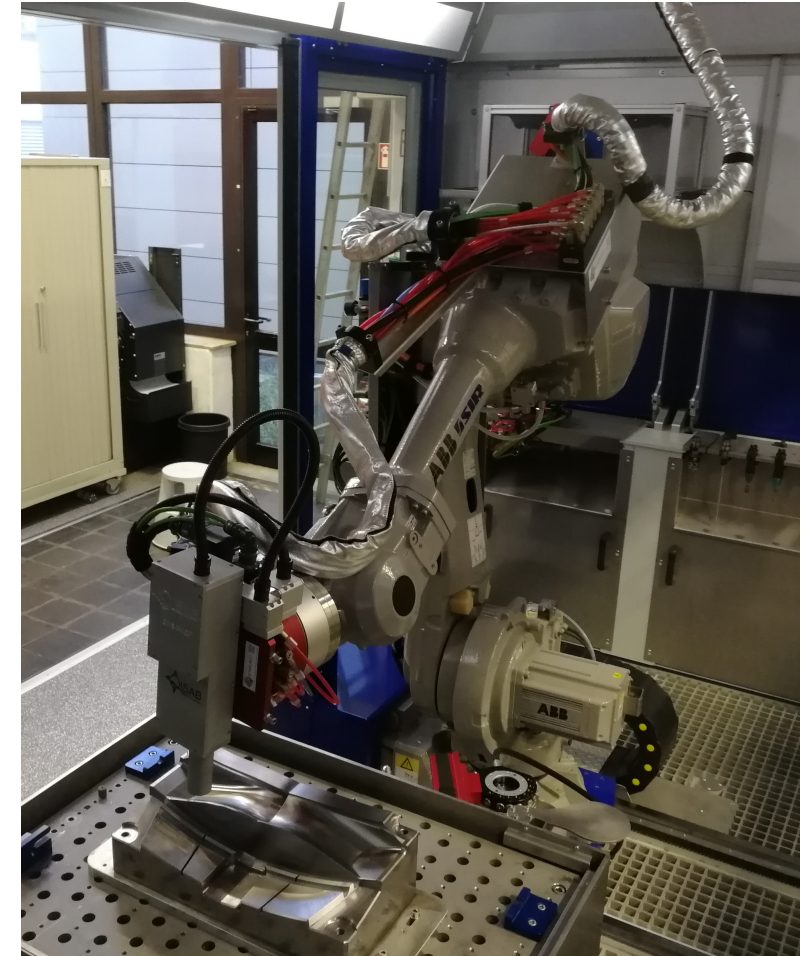
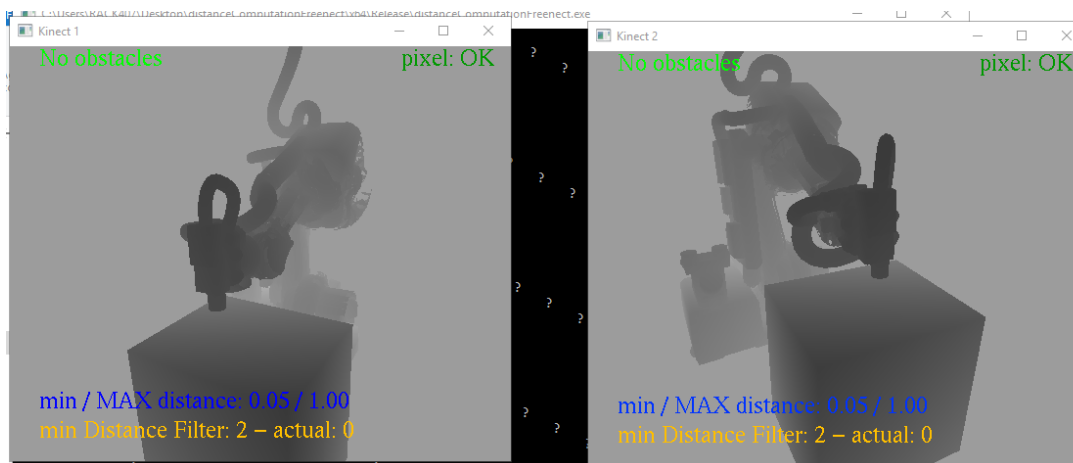
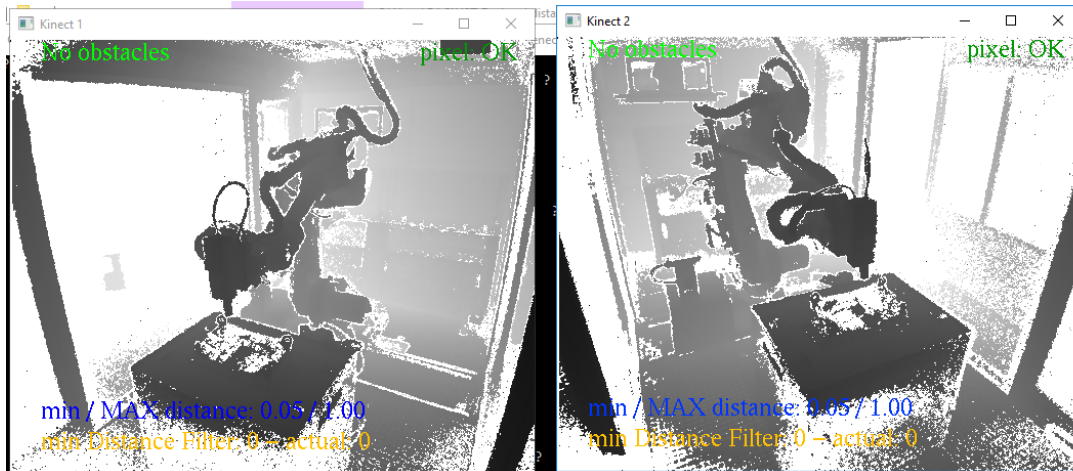
Considering **CWS** laser measuring device, cables or other equipment in distance computation

CWS =  
Coherent Wave Scattering



SYMPLEXITY

H2020 FoF EU project (2015-18)

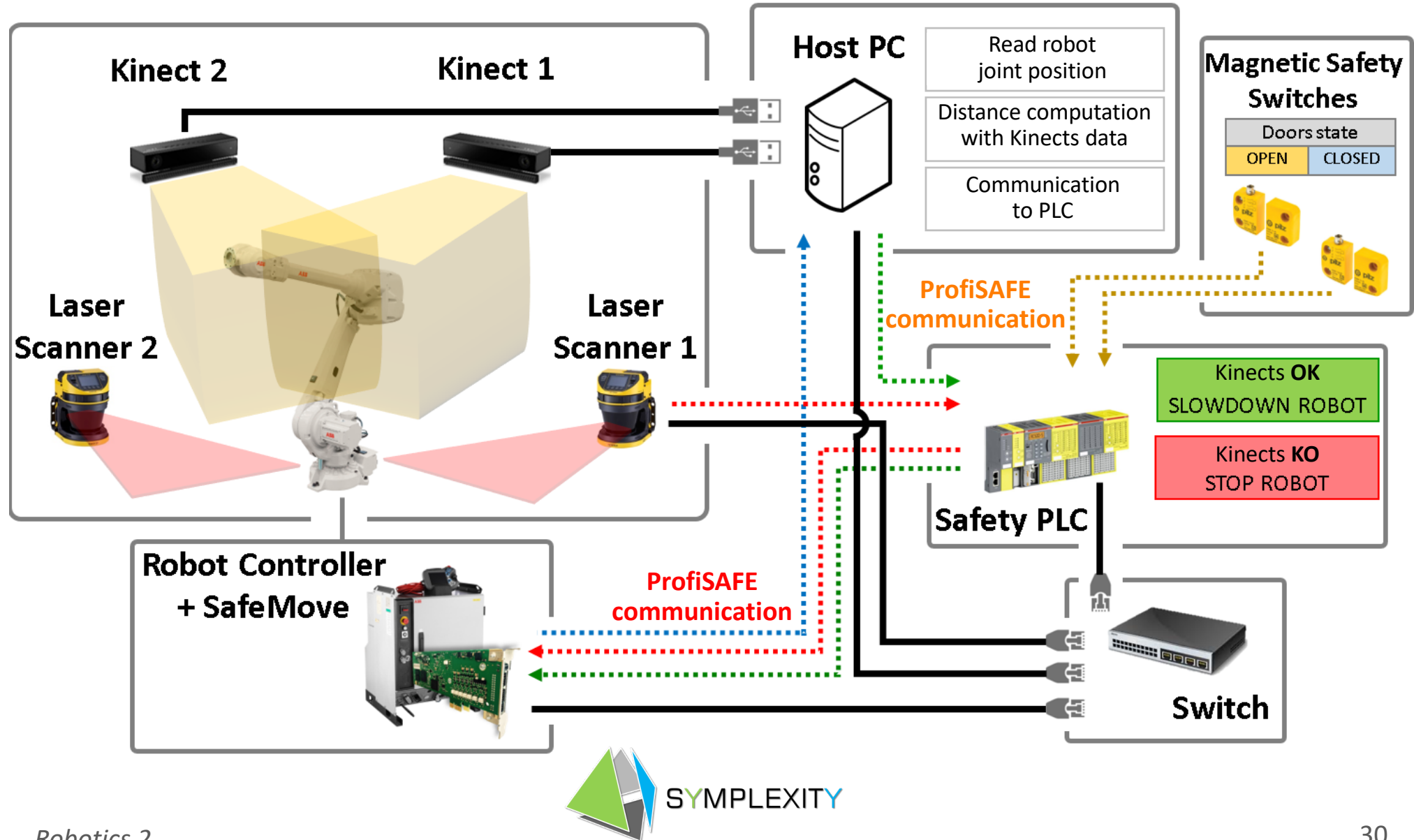


for each robotic set up, the suitable CAD model for depth space subtraction is loaded at start



# Implemented control and communication architecture

Two **Kinects** for accurate HR distance monitoring, two **laser scanners** for backup safety





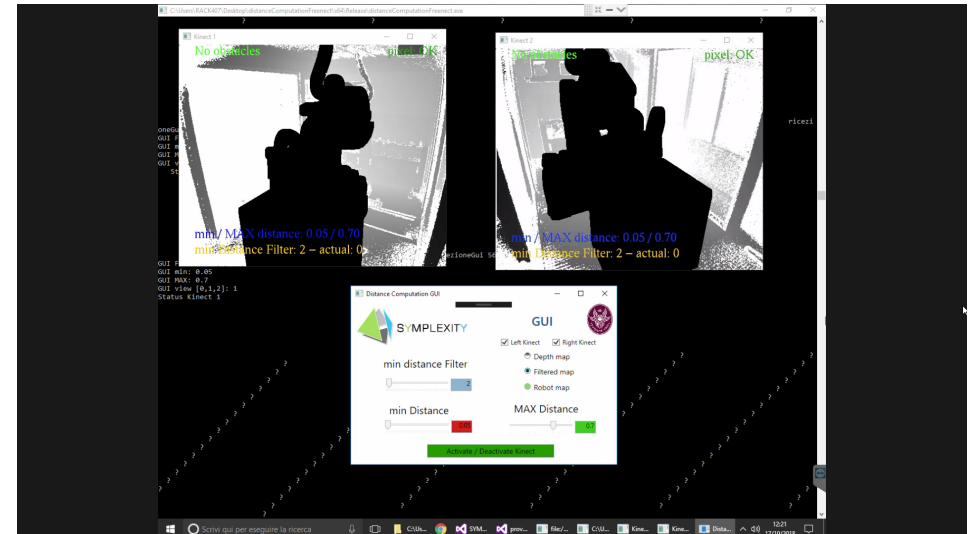
# Safe coexistence in an industrial robotic cell

ABB IRB 4600 operation in an abrasive finishing cell with **human access**

video



video



depth images and GUI

- robot is moving at max 100 mm/s
- no safety zones were defined in ABB SafeMove
- Kinects **OK** (except when the view of one of the cameras is obstructed on purpose)





# Collaboration

Contactless or physical

---

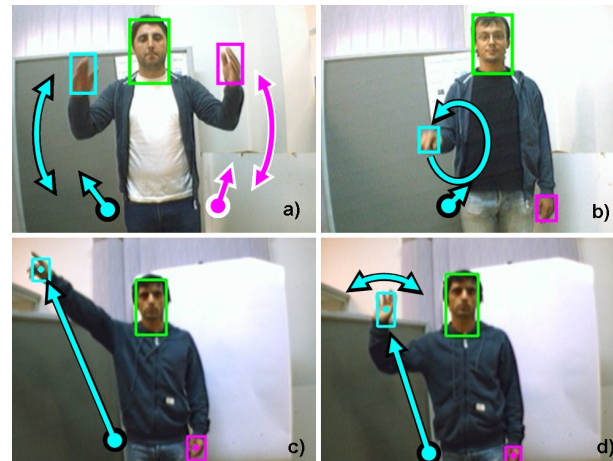
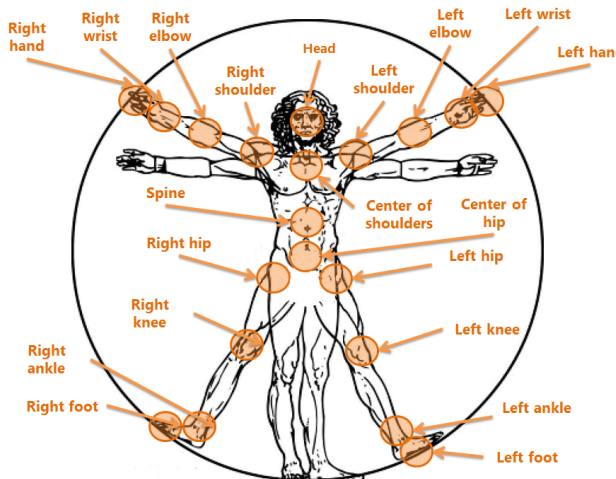
- in **contactless** collaboration, robot (or human!) actions are guided or follow from an exchange of information without physical interaction
  - this can be achieved via **direct communication**, e.g., with gestures and/or voice commands
  - or via **indirect communication**, by recognizing human intention or attention, e.g., through eye gaze
  - another form is **visual coordination** in which vision is used to coordinate human-robot relative motion
- in **physical** collaboration, there is an explicit and intentional contact with exchange of forces between human and robot
  - by measuring or **estimating contact forces**, the robot can predict human motion intention and react accordingly to it
  - collaborative tasks (e.g., human and robot carrying a heavy object) require **control of exchanged forces (and motion)** at the contact



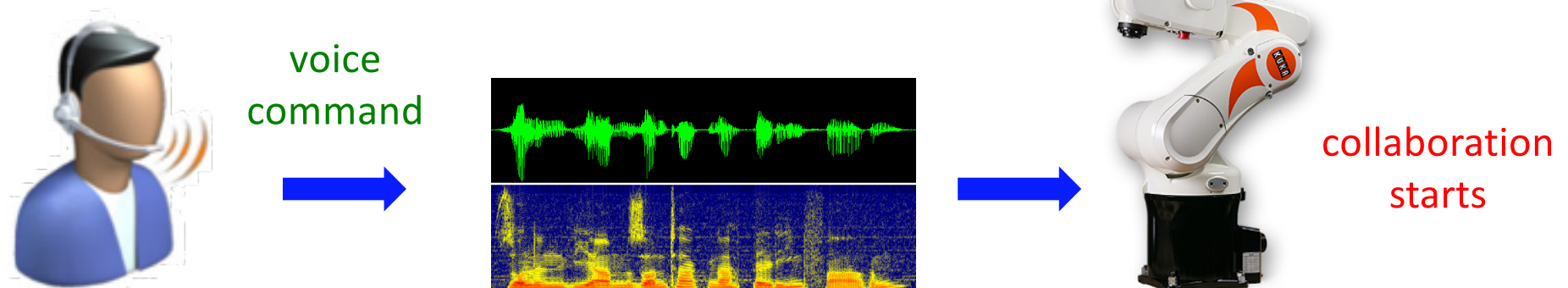
# Contactless collaboration

Using gesture and voice commands

- human body parts and gesture recognition



- speech recognition





# Human-robot communication

Using Kinect and SDK library

- the robot end-effector **position** is commanded by voice/gestures to **follow** (or **go to**) the human **left, right, or nearest hand**





# Gesture communication in SYMPLEXITY cell

Using Kinect 2.0 RGB-D sensor, with built-in skeleton tracking



- initial 5 sec gesture to activate
- both hands **open** = start motion
- both hands **closed** = stop robot
- left closed + right open = limit speed
- left open + right closed = recover speed
- final gesture to deactivate

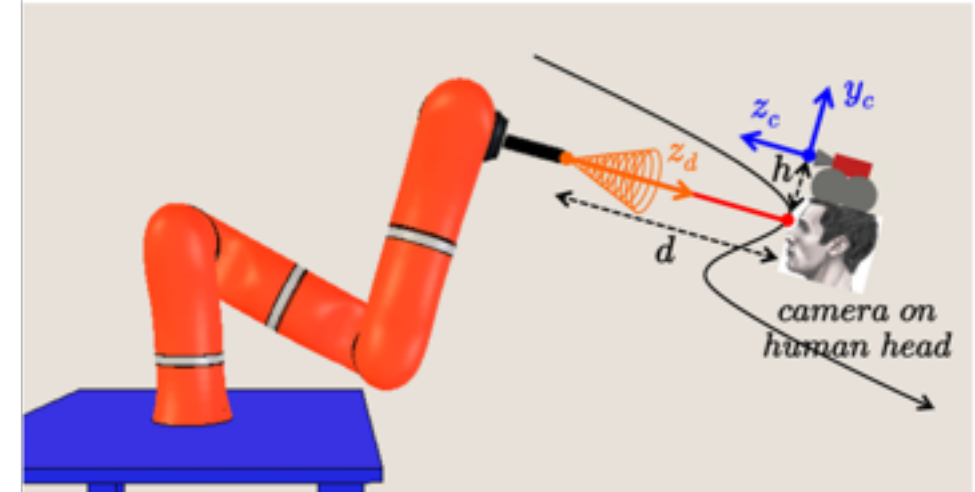
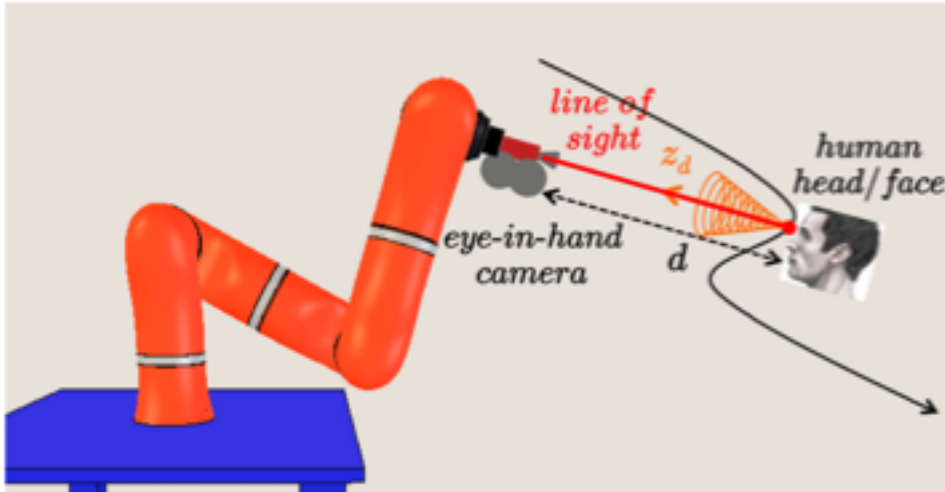


video



# Visual coordination task

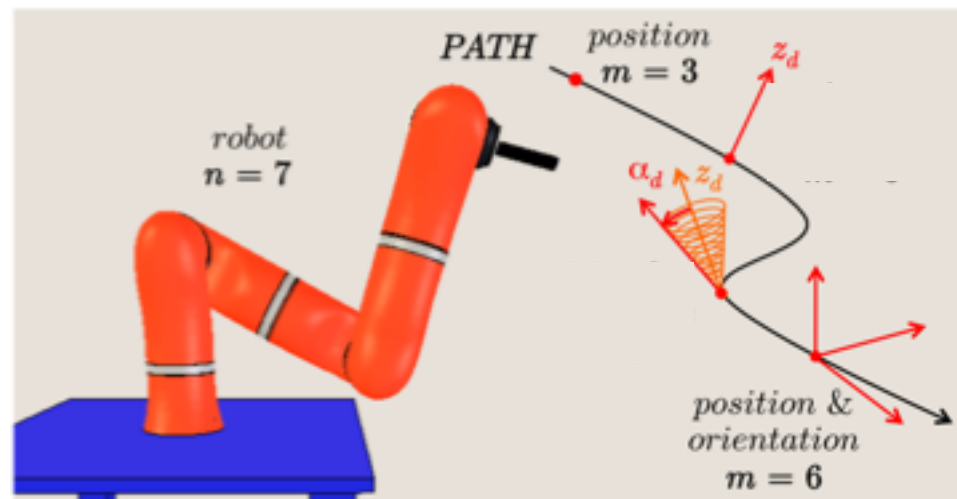
Dual formulations of human-robot relative tracking (IROS 2017)



- camera **on robot**, pointing to moving human head/face kept at a certain relative position
- camera **on human head**, with robot pointing to it and kept at a certain relative position

different Cartesian motion tasks  
of varying dimension  $m \leq n$

cone represents a **relaxation**  
of the pointing task by some  
relative angle  $\alpha_d$



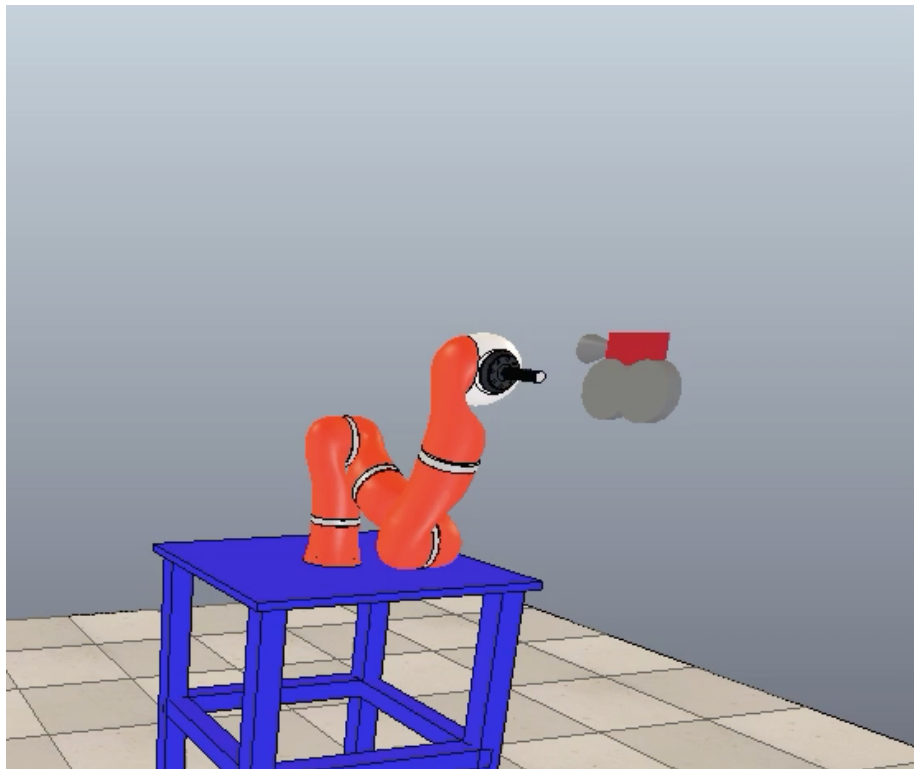


# Simulation

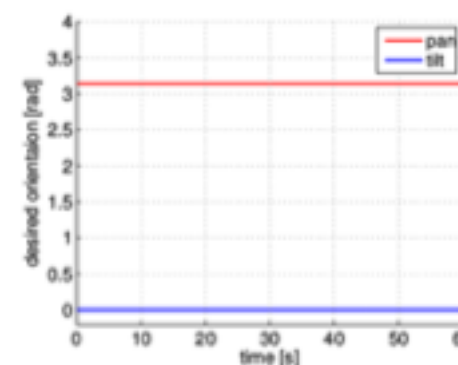
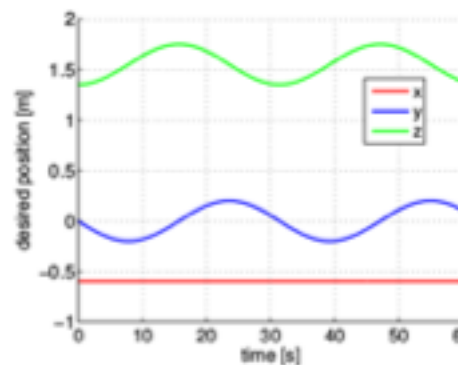
Motion control using Task Augmentation method

- camera **tracing a circle** in a vertical plane, while **pointing** direction is kept **constant**

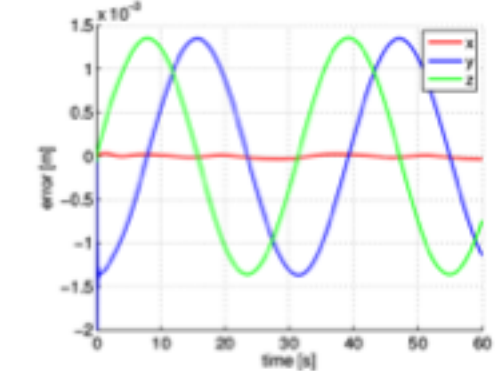
ROS environment, integrated with robot simulator **V-REP**



video



position errors < 1.5 mm



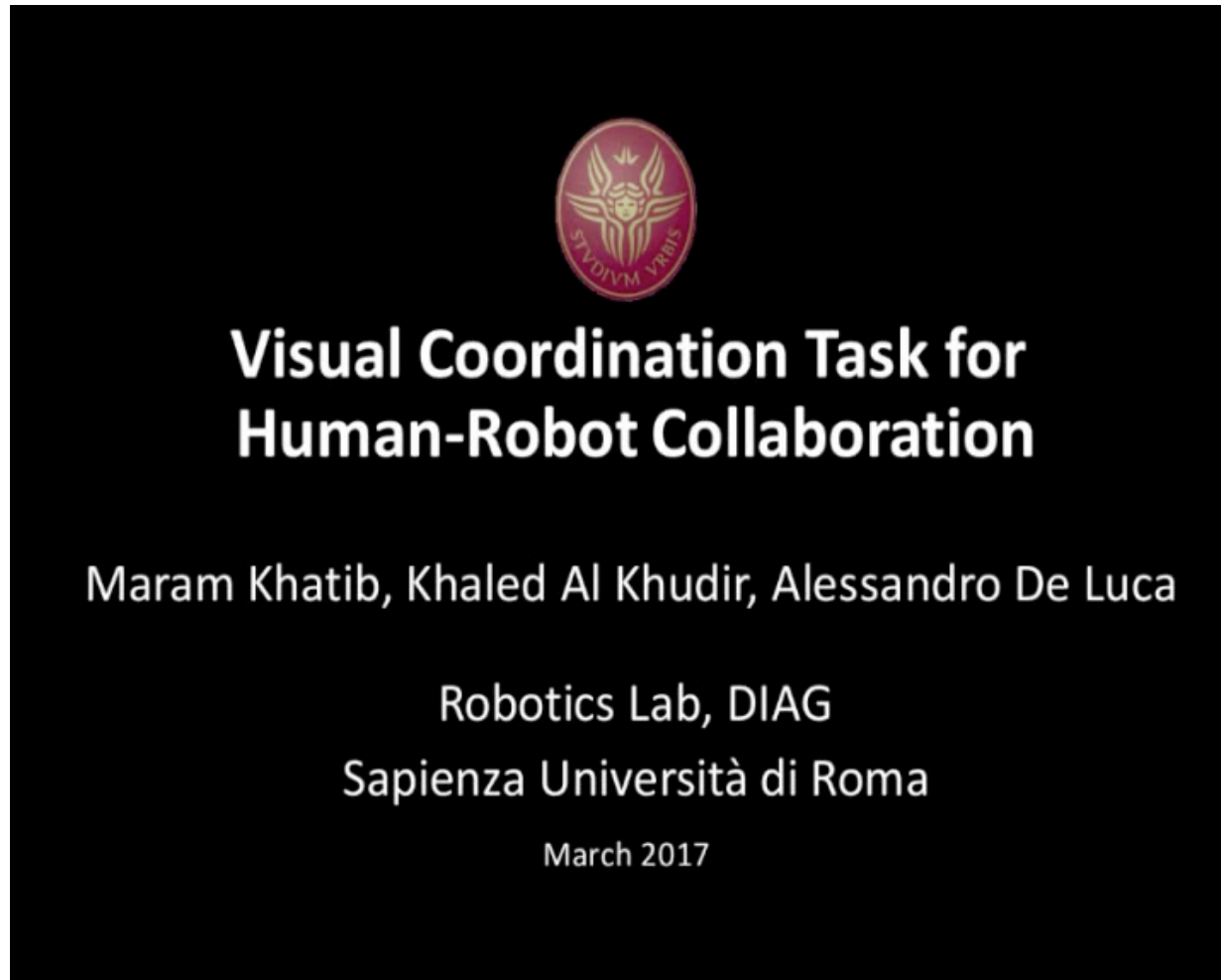
pointing error < 0.006



# Experiment of visual coordination

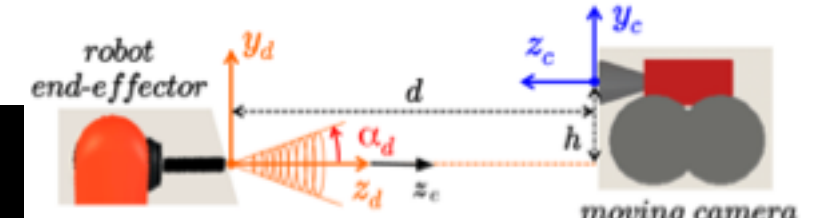
KUKA LWR robot in ROS environment with FRI

<https://youtu.be/SRfpNrZD7k0>



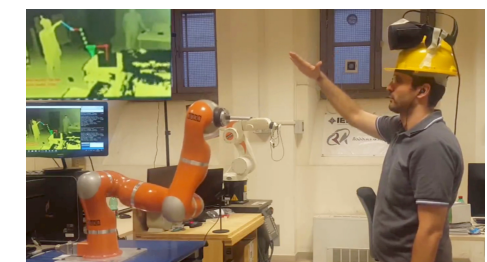
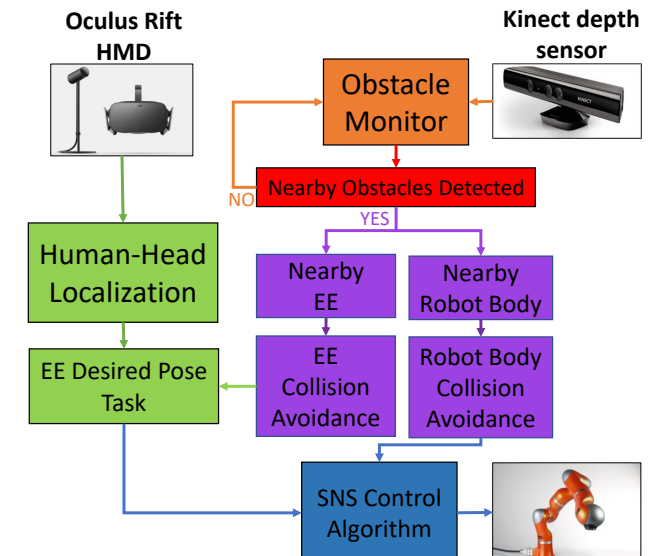
Robotics 2

video



position error  $\leq 5$  cm   pointing error  $< 0.03$  rad

also in multi-sensory operation

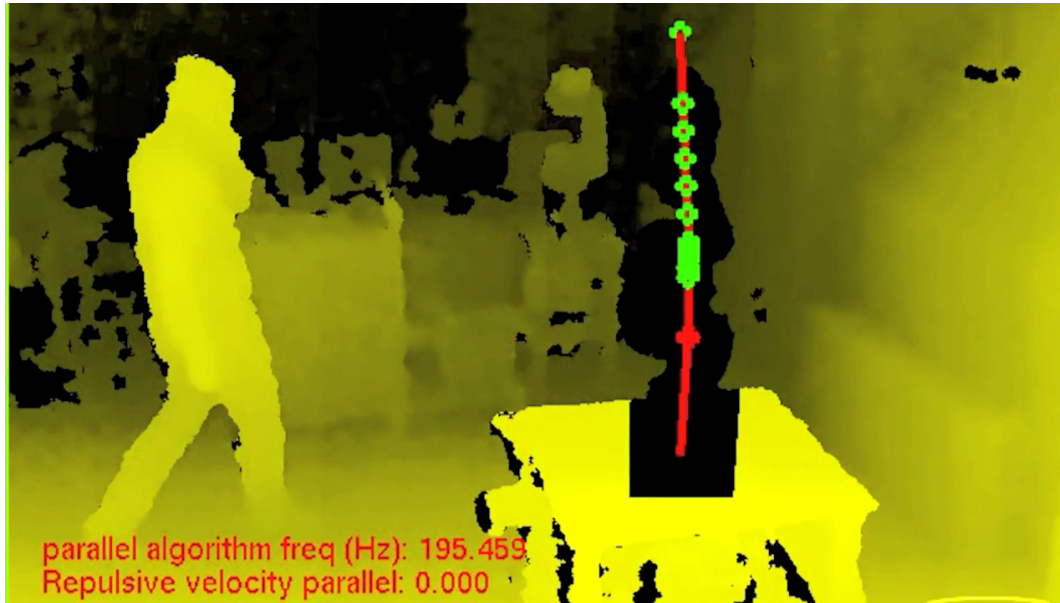


38



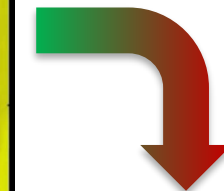
# Safe human-robot interaction

From coexistence to physical collaboration



video

**coexistence** through  
collision avoidance



<https://youtu.be/pIIhY8E3HFg>

**physical collaboration** through  
contact identification  
(here, end-effector only)



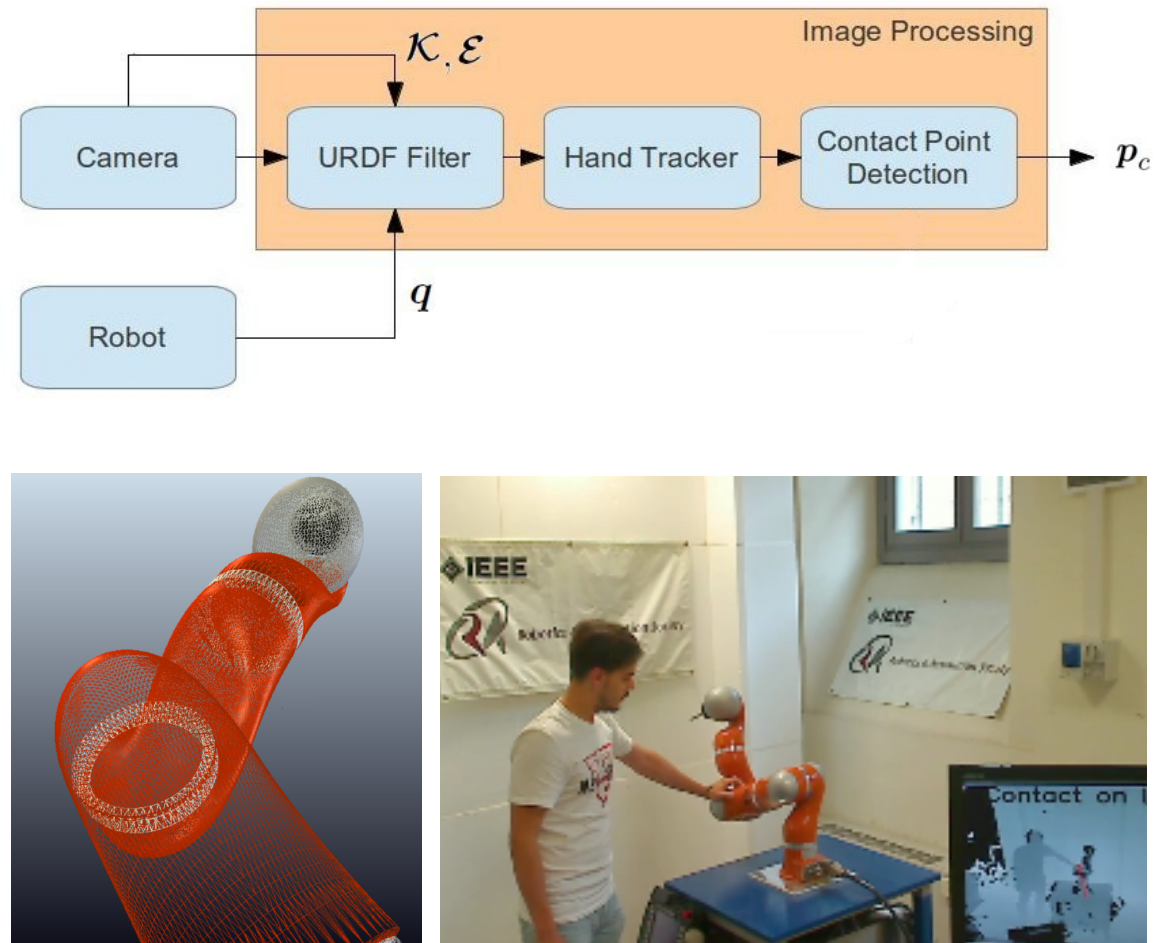
video



# Distance and contact point localization

Using Kinect, CAD model, and distance computation to **localize contact** (early 2014)

- **depth image** is acquired by a Kinect
- robot is removed from image (URDF filter by TUM), starting from its 3D CAD model
- human hand tracking on filtered image
- **3D CAD model of robot** and hand position are used to localize contact point on robot surface
- surfaces of robot links are modeled using polygonal patches
- 3D robot model is projected in workspace with a calibration matrix
- **distances are computed** between vertices of patches and the human hand
- ranges vary from about 20 cm (area of interest) down to 0 (contact)
- **residuals** are always zero when robot moves in free space





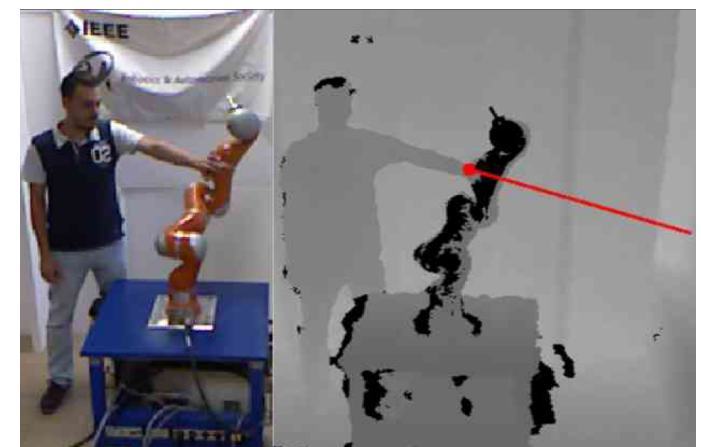
# Distance and contact point localization

Use **residuals** to detect the contact event, also for multiple locations

- when the **residual** indicates a **contact/collision** (and colliding link), the **vertex** in the robot CAD surface model **with minimum distance** is taken as the **contact point**
- algorithm applied here in parallel to both **left** and **right** hand (no other body parts)



video

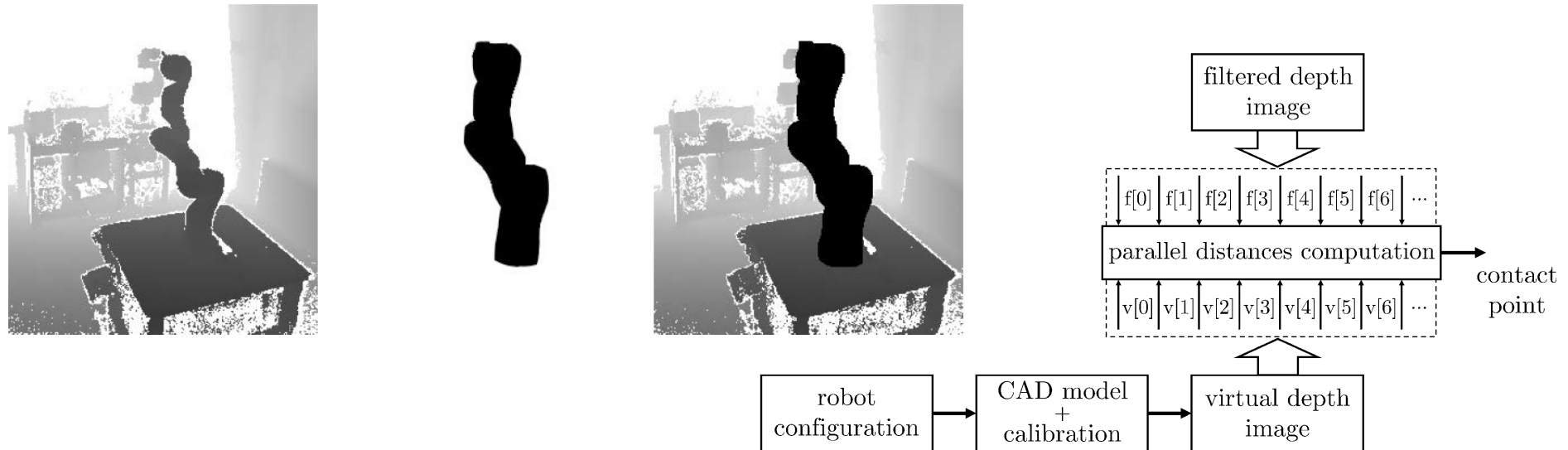




# Improved contact point localization

Real-time localization using the CUDA framework (IROS 2017)

- the algorithm, based on distance computation in **depth space**, takes advantage of a **CUDA framework** for massively parallel **GPU** programming; **three 2.5D images** are processed:
  - real depth image  $I_r$ , captured by a RGB-D sensor (a Kinect)
  - virtual depth image  $I_v$ , containing only a projection of the robot CAD model
  - filtered depth image  $I_f = f(I_r, I_v)$ , containing only the obstacles



- parallel **distance computations** between **all robot points** in virtual image and **all obstacle points** in filtered image (same time needed to localize one or multiple contact points!)



# Contact force estimation

Combining internal and external sensing

## ■ task

- localize (in the least invasive way) points on robot surface where contacts occur
- estimate exchanged **Cartesian** forces
- control the robot to react to these forces according to a desired behavior

## ■ solution idea

- use residual method to **detect** physical contact, **isolate** the colliding link, and **identify** the joint torques associated to the external contact force
- use a depth sensor to **classify** the human parts in contact with the robot and **localize** the contact points on the robot structure (and the **contact Jacobian**)
- **solve** a linear set of equations with the residuals, i.e., estimates of joint torques resulting from **contact wrenches** (**forces/moments**) applied anywhere to the robot

$$\boldsymbol{r} \simeq \boldsymbol{\tau}_{ext} = \boldsymbol{J}_c^T(\boldsymbol{q})\boldsymbol{\Gamma}_c = \begin{pmatrix} \boldsymbol{J}_{L,c}^T(\boldsymbol{q}) & \boldsymbol{J}_{A,c}^T(\boldsymbol{q}) \end{pmatrix} \begin{pmatrix} \mathbf{F}_c \\ \mathbf{M}_c \end{pmatrix}$$



# Contact force estimation

## Some simplifying assumptions

- dealing with contact forces
  - most **intentional** contacts with a single human part (hand, arm, fingers) are **not** able to transfer relevant **torques**
  - to estimate reliably  $\Gamma_c$  we should have rank  $J_c = 6$ , which is true only if the robot has  $n \geq 6$  joints and the contact occurs at a link with index  $\geq 6$

assume   $M_c = 0$

only a **pure Cartesian force** is considered

- dimension of the task related to the contact force is now  $m = 3$  and its **estimation** is

$$r \simeq \tau_{ext} = J_{Lc}^T(q) F_c \quad \rightarrow \quad \hat{F}_c = (J_{Lc}^T(q))^\# r$$

- the contact Jacobian can be evaluated once the contact point is detected by the external depth sensor that closely monitors the robot workspace
- this procedure represents a so-called **virtual force sensor**



# Validation of virtual force sensor

Experiments in **static** conditions with the KUKA LWR 4 (IROS 2014)



- evaluation of estimated contact force

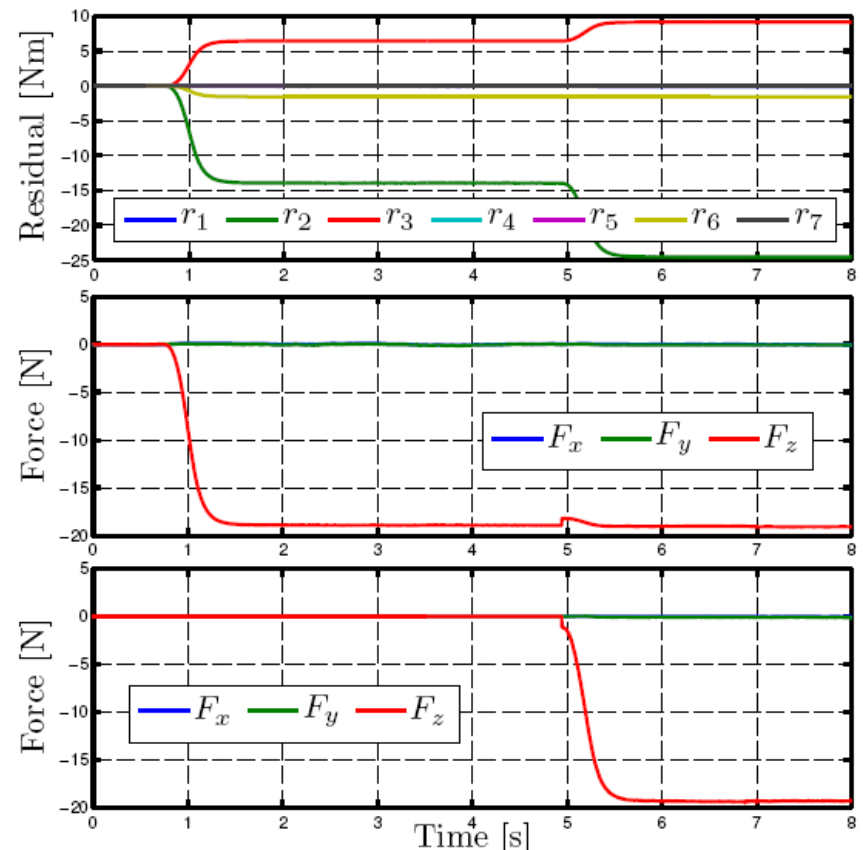
$$\hat{\mathbf{F}}_c = (\mathbf{J}_c^T(\mathbf{q}))^\# \mathbf{r}$$

- estimation accuracy was initially tested using known masses in known positions
- a single mass hung either on link 4 or on link 7, to emulate a **single** (point-wise) contact

Link #	Mass	$F_z$	using $\mathbf{J}_{Lc}$		using $\mathbf{J}_c$	
			$\hat{F}_z$	Deviation	$\hat{F}_z$	Deviation
4	1.93	-18.93	-18.75	0.95%	-4.46	76.43%
7	1.93	-18.93	-18.91	0.1%	-18.82	0.58%

- a mass hung on link 7, and then a second on link 4 so as to emulate a **double** contact

Link #	Mass	$F_z$	$\hat{F}_z$	Deviation
4	2.03	-19.91	-19.43	2.41%
7	1.93	-18.93	-19.04	0.58%



case of two masses



# On-line estimation of contact force

Used within an admittance control scheme (IROS 2014)

<https://youtu.be/Yc5FoRGJsrc>

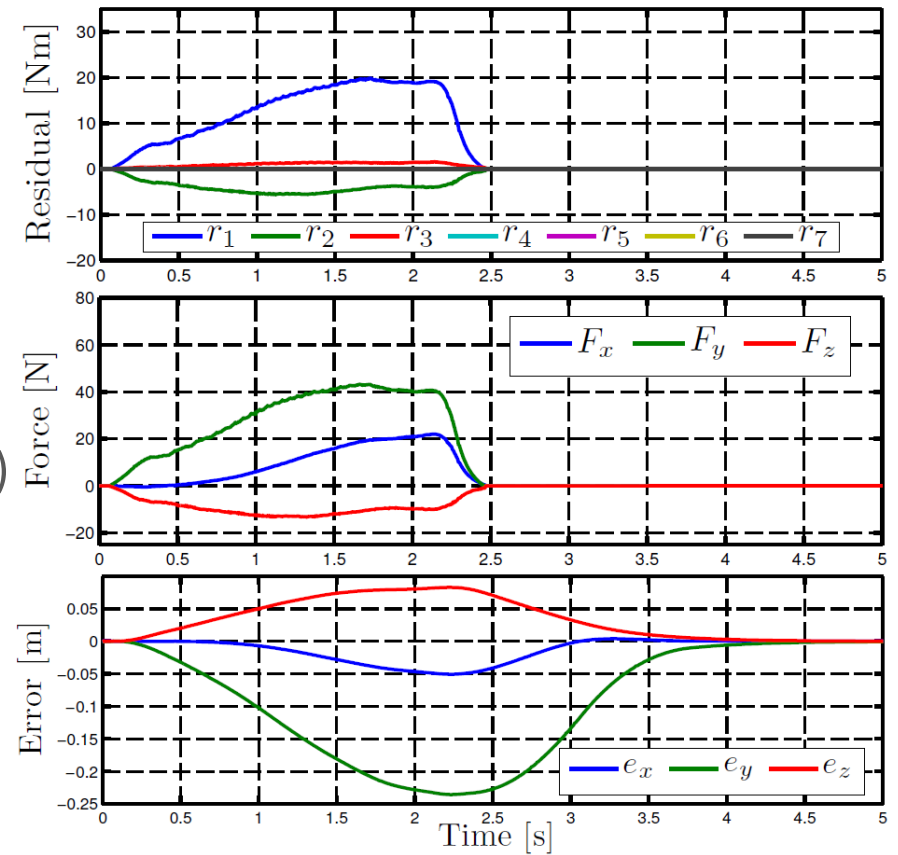
The video thumbnail features the Sapienza Università di Roma logo at the top center. Below it is the title 'Estimation of Contact Forces using a Virtual Force Sensor' in large white font. Underneath the title, the names 'Emanuele Magrini, Fabrizio Flacco, Alessandro De Luca' are listed. At the bottom, the text 'Dipartimento di Ingegneria Informatica, Automatica e Gestionale, Sapienza Università di Roma' is displayed, along with the date 'February 2014'. In the bottom right corner of the thumbnail, the word 'video' is written in green.



# On-line estimation of contact force

Evolution of residuals, estimated forces, and compliant displacements

- control gains are chosen so as to assign a **stiff** behavior at a reference configuration
- at some time, human pushes on robot link 3
- due to the stiff robot behavior, a large force needs to be applied to move the robot
- when the hand is removed, the contact point returns smoothly to its initial position (zero error)



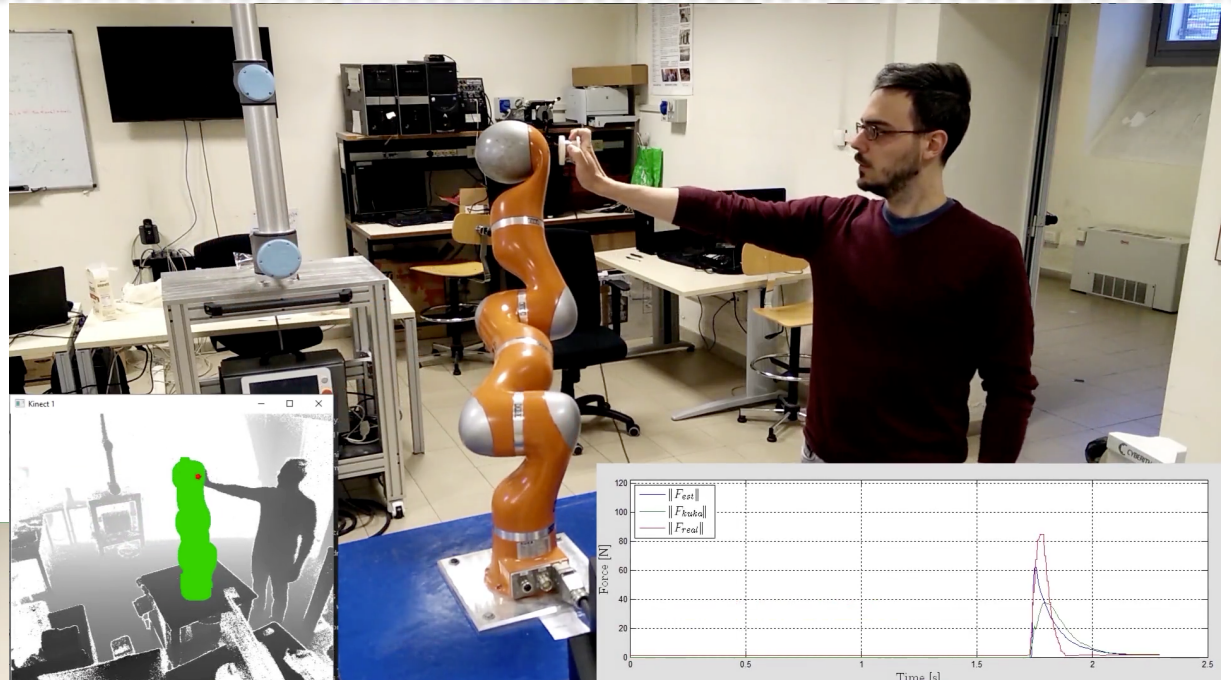
see slide #54 for the chosen  
**admittance control** scheme



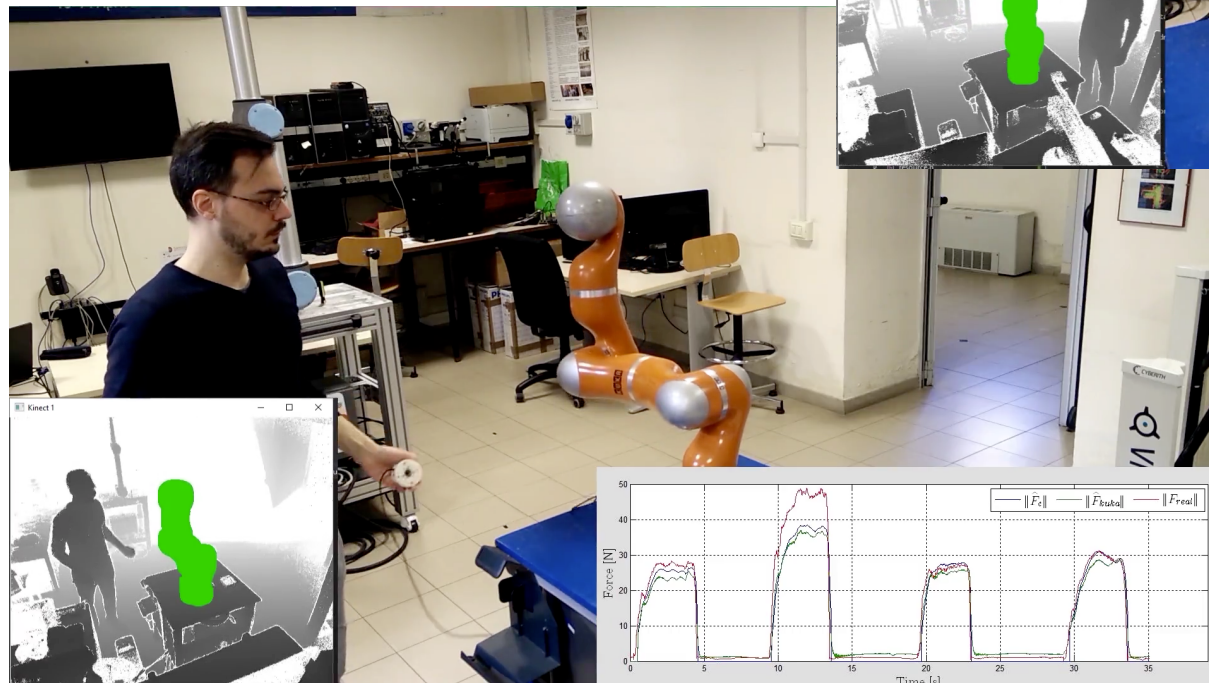
# Further validation of virtual force sensor

In static and **dynamic** conditions, using a hand-held F/T sensor (February 2019)

- comparing the F/T ground truth contact force measure with its residual-based estimation
  - with robot **at rest** (pushing)
  - in **robot motion** (hitting)



video



outgrowth of Emanuele Magrini's PhD thesis, May 2016

video



# Estimation of contact force

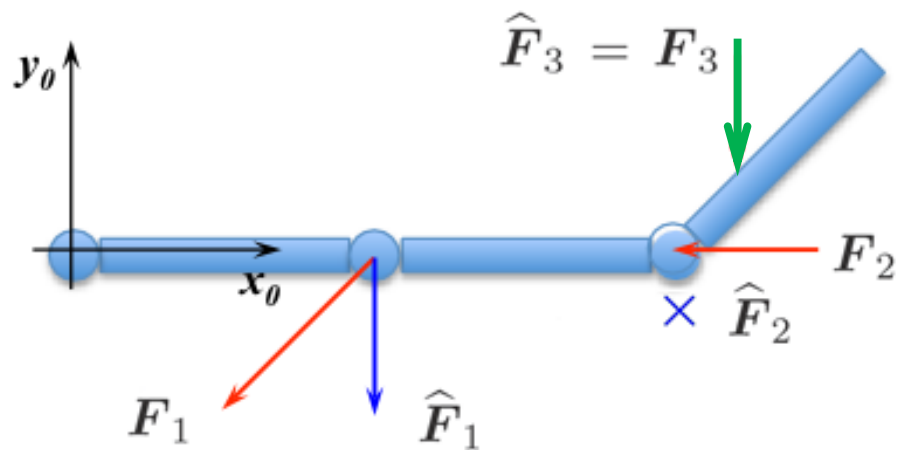
Some limitations of the residual method

- **multiple** simultaneous contacts can be considered (e.g., with **both** human hands)

$$\begin{pmatrix} \hat{\mathbf{F}}_1 \\ \hat{\mathbf{F}}_2 \end{pmatrix} = (\mathbf{J}_{L1}^T(\mathbf{q}) \ \mathbf{J}_{L2}^T(\mathbf{q}))^\# \mathbf{r}$$

but with much **less confidence** in the resulting force estimates (**detection is still ok**)

- **estimates** will be limited only to those components of  $\mathbf{F}_c$  which can be detected by the residual (i.e., that produce work on robot motion)
- all **forces**  $\mathbf{F}_c \in \mathcal{N}(\mathbf{J}_c^T(\mathbf{q}))$  will never be recovered  $\Leftrightarrow$  they are ‘absorbed’ by the robot structure

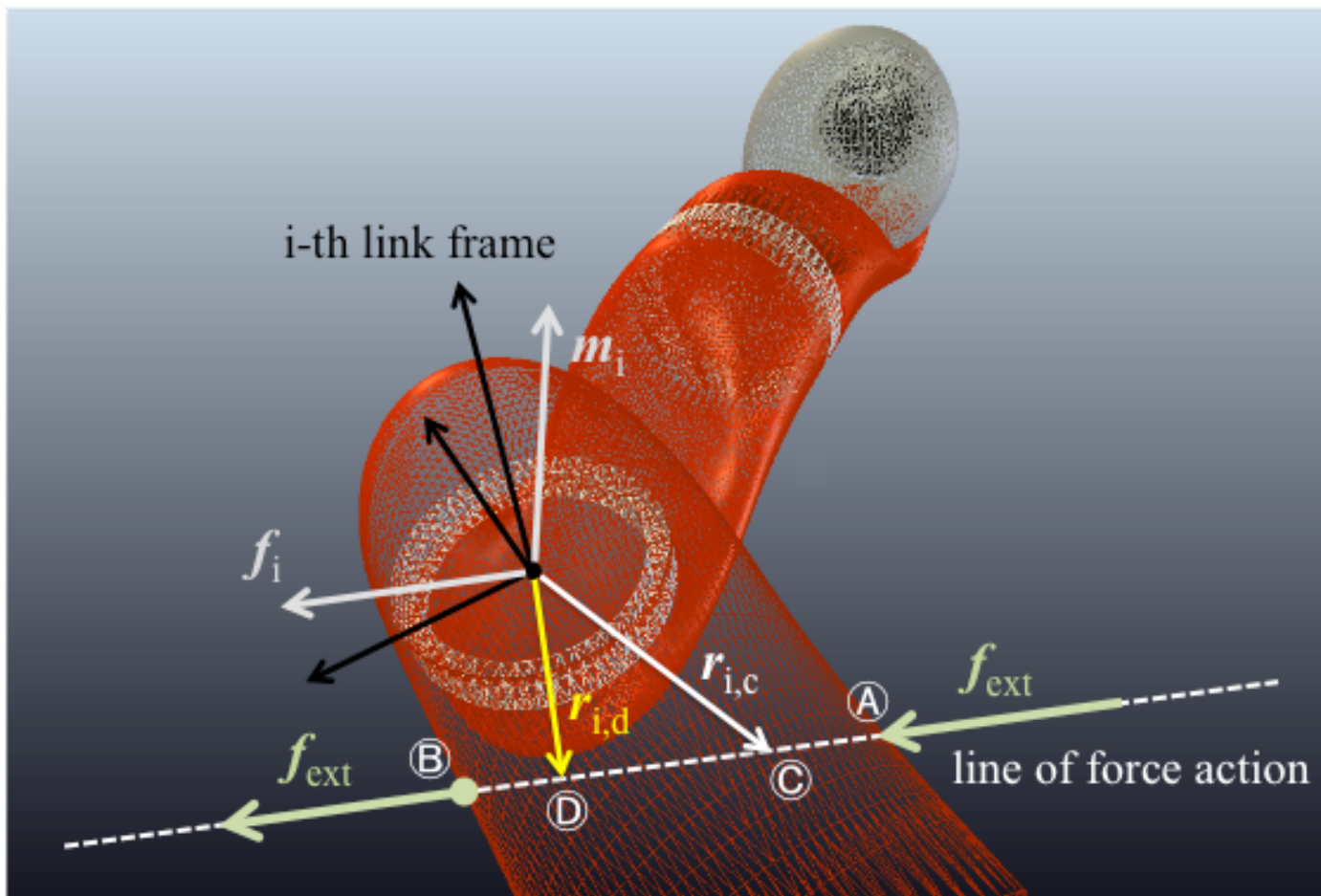




# Estimation of contact force

Sometimes, even **without** external sensing

- if contact is sufficiently “down” along the kinematic chain ( $\geq 6$  residuals available), the estimation of **pure contact forces** does not need any external information ...

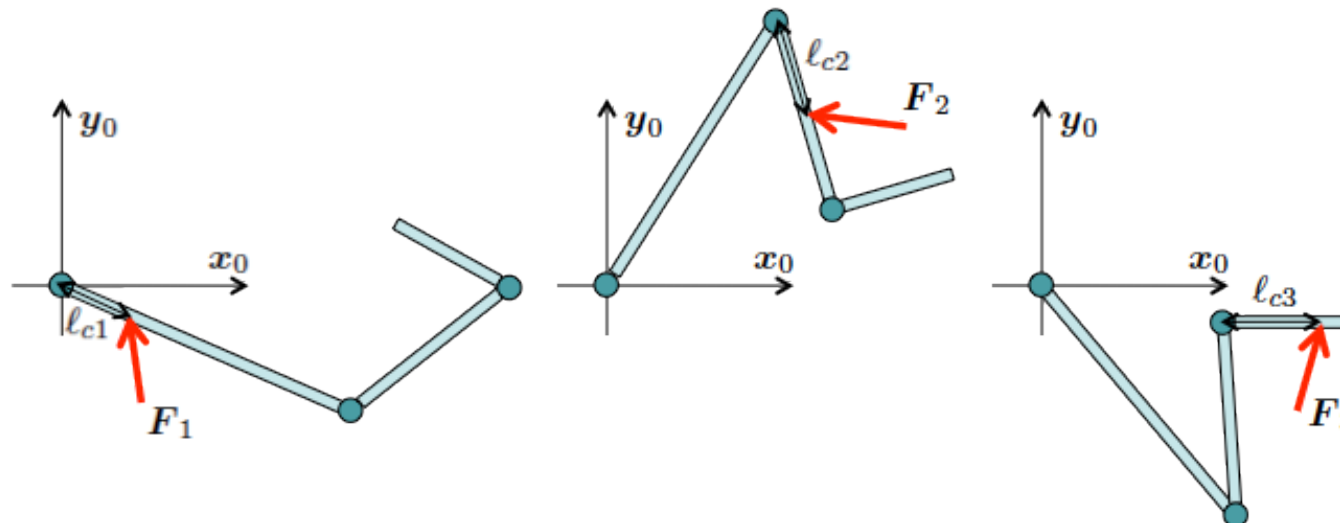




## A closer analysis

Which force components are being estimated? Do we really need **external** sensing?

- a simple 3R planar case, with contact on different links



$r$  is a vector of dimension 3

$$\text{rank} \{ J_{c1} \} = 1$$

$$\text{rank} \{ J_{c2} \} = 2$$

$$\text{rank} \{ J_{c3} \} = 2$$

$\hat{F}_i$  {  
only **normal** force to link,  
if contact point is known  
(1 informative residual signal)}

full force on link,  
if contact point is known  
(2 informative residuals)

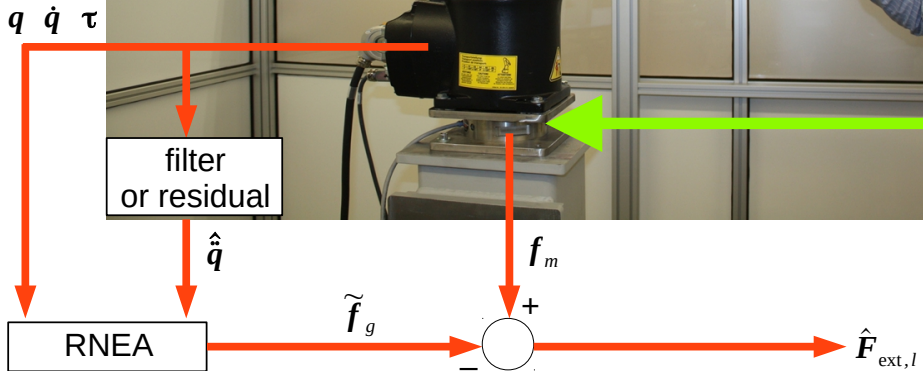
full force on link, **even**  
**without** knowing contact  
(3 informative residuals)

- forces  $F_k \in \mathcal{N}(J_k^T(q))$  will never be recovered (**even** with known contact)

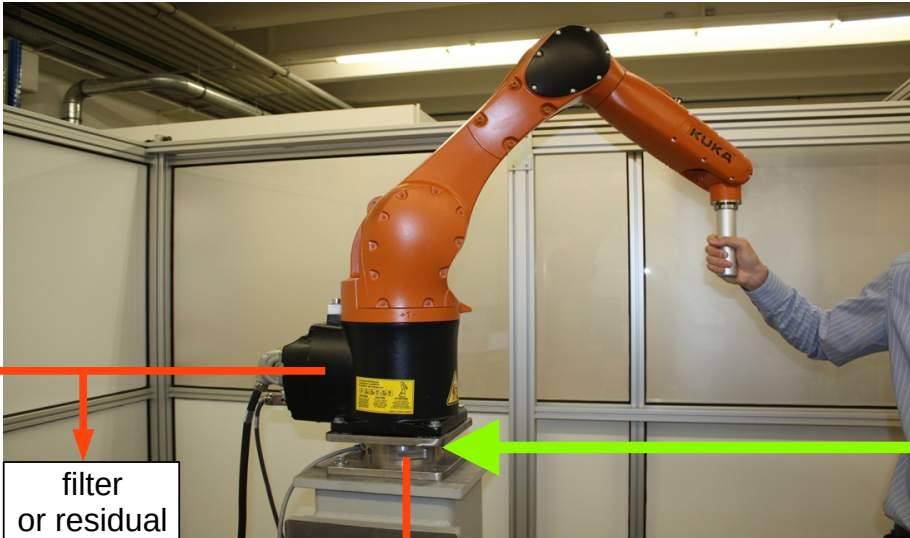


# Additional F/T sensor at the base

Combining real & virtual sensors for estimating interaction forces/moment (IROS 2016)



- an external wrench acting on link  $l$  will only affect the first  $l$  components of  $\tau_{ext}$
- effect of  $F_{ext}$  on  $\tau_{ext}$  depends on point  $p_l$  while that of  $M_{ext}$  does not, since **only** the contact link is relevant (isolated by residual)



KUKA 6-dof Agilus robot (@Augsburg)

- Recursive Newton-Euler Algorithm (fed by the residuals) for **ground force/moment** prediction
- comparison with **base F/T sensor readings**

(large) F/T sensor mounted at the base

Table of possible options/improvements  
for a contact wrench  $W_{ext,l} = (F_{ext,l}, M_{ext,l})$

	$l$	Known $p_l$	Unknown $p_l$ with pure contact force
<b>F/T</b> sensor at the base	any	Estimate $W_{ext,l}$	Estimate $F_{ext,l}$ and $p_l$
<b>F</b> sensor at the base	any	Estimate $F_{ext,l}$	Estimate $F_{ext,l}$
	$\geq 3$	Estimate $W_{ext,l}$	Estimate $F_{ext,l}$ and $p_l$
<b>No</b> sensor at the base	$\geq 6$	Estimate $W_{ext,l}$	Estimate $F_{ext,l}$ and $p_l$



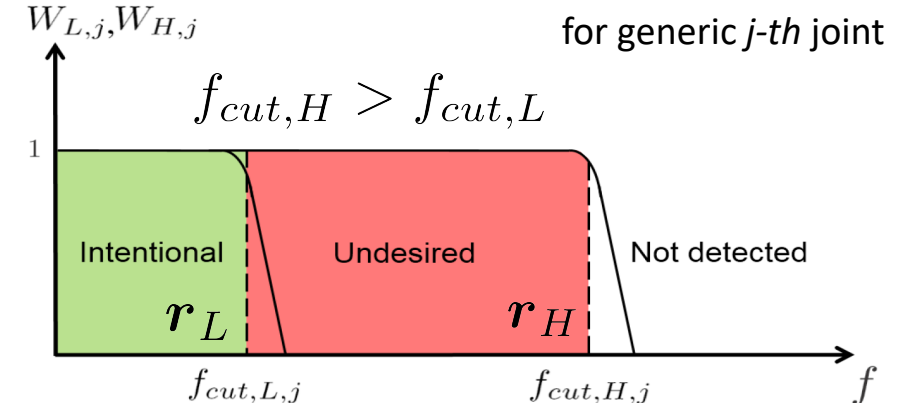
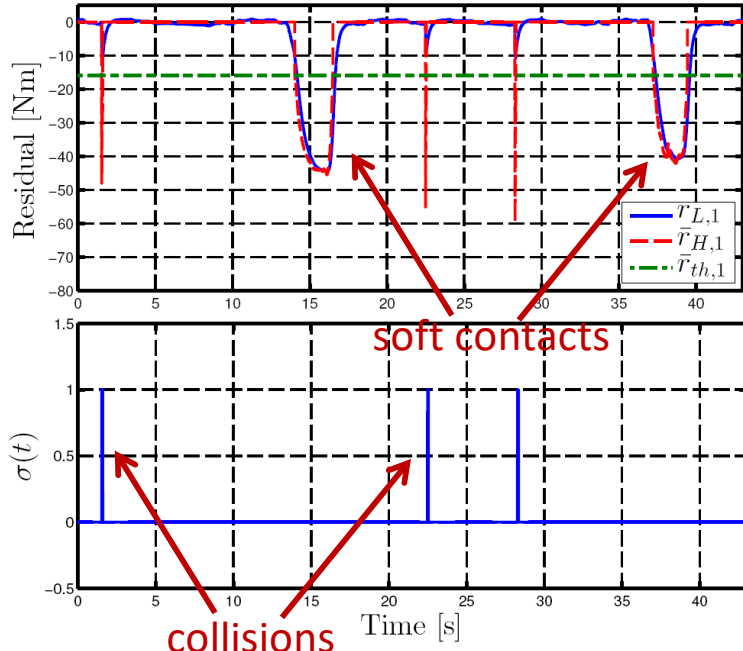
# Collision or collaboration?

Distinguishing **hard/accidental** collisions and **soft/intentional** contacts

- using suitable **low** and **high** bandwidths for the residuals (first-order stable filters)

$$\dot{r} = -K_I r + K_I \tau_K$$

- a **threshold** is added to prevent false collision detection during robot motion



video



# Collaboration control

Use of estimate of the external contact force for control (e.g., on a Kuka LWR)

- shaping the robot dynamic behavior in specific **collaborative tasks** with human
  - joint carrying of a load, holding a part in place, whole arm **force** manipulation, ...
  - robot motion controlled by
    - **admittance** control law (in **velocity FRI mode**)
    - **force**, **impedance** or **hybrid force-motion** control laws (needs **torque FRI mode**)
- all implemented **at contact level**
- e.g., admittance control law using estimated contact force (as in video of slide #46)
  - the scheme is realized at the single (or first) contact point
  - desired **velocity** of contact point taken proportional to (**estimated**) contact force

$$\dot{\mathbf{p}}_c = \mathbf{K}_a \mathbf{F}_a, \quad \mathbf{K}_a = k_a \mathbf{I} > 0$$

$$\mathbf{F}_a = \hat{\mathbf{F}}_c + \mathbf{K}_p (\mathbf{p}_d - \mathbf{p}_c), \quad \mathbf{K}_p = k_p \mathbf{I} > 0$$

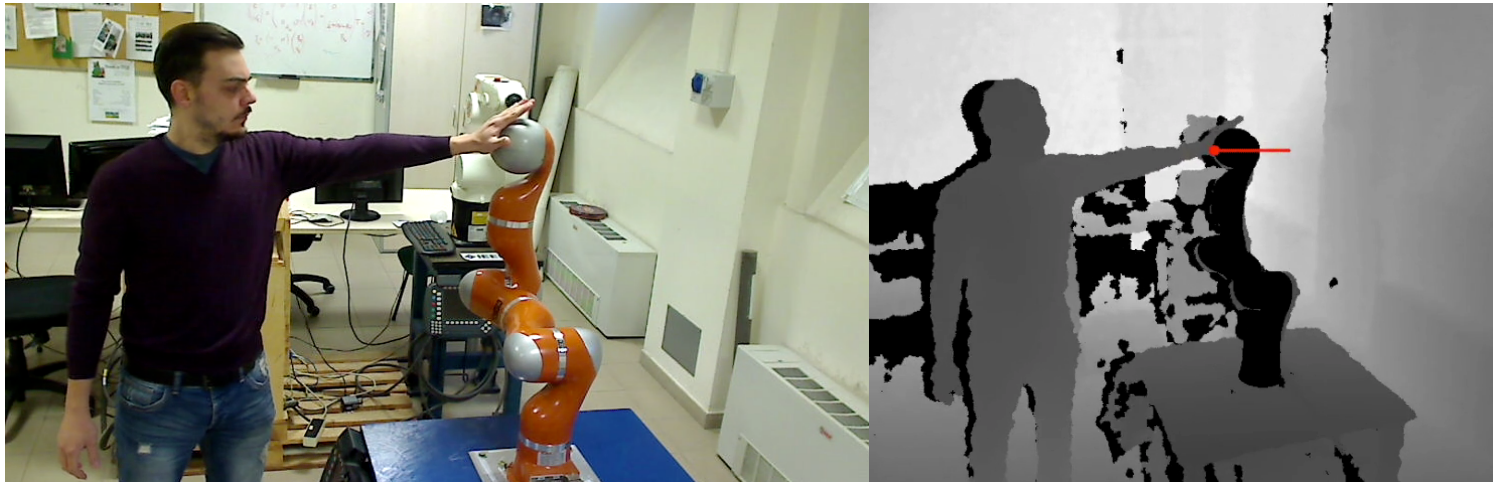
initial contact point position when interaction begins



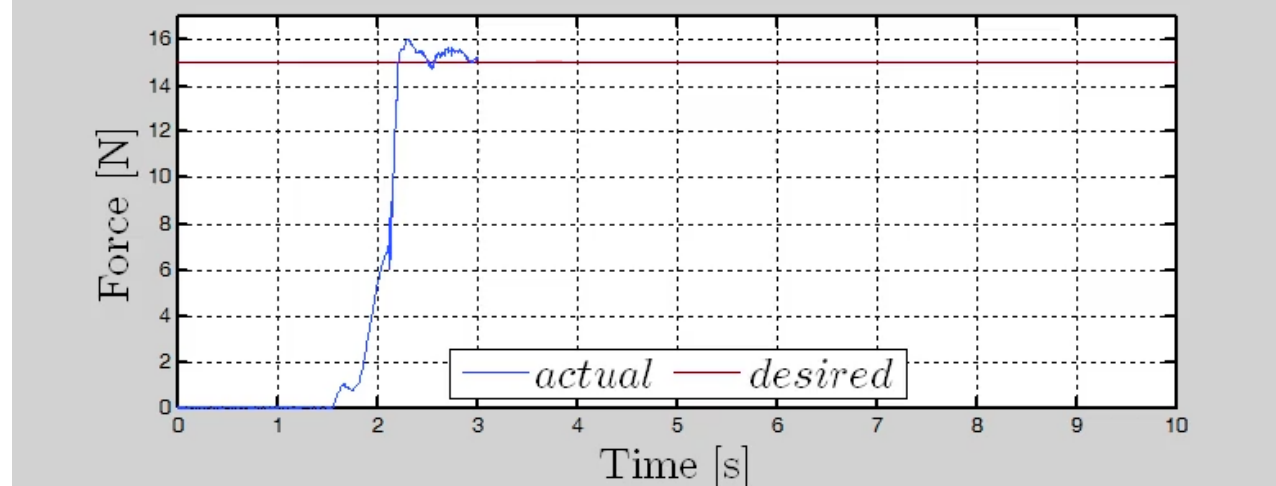
# Contact force regulation with virtual force sensing

Human-robot collaboration in torque control mode (ICRA 2015)

- contact force estimation & control (anywhere/anytime)



video



see ICRA 2015

trailer (at 3'26''):

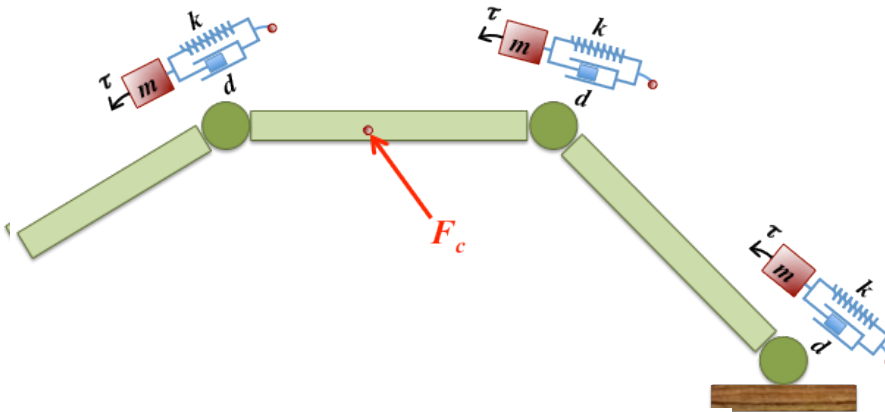
<https://youtu.be/glNHq7MpCG8> (Italian); [https://youtu.be/OM\\_1F33fcWk](https://youtu.be/OM_1F33fcWk) (English)



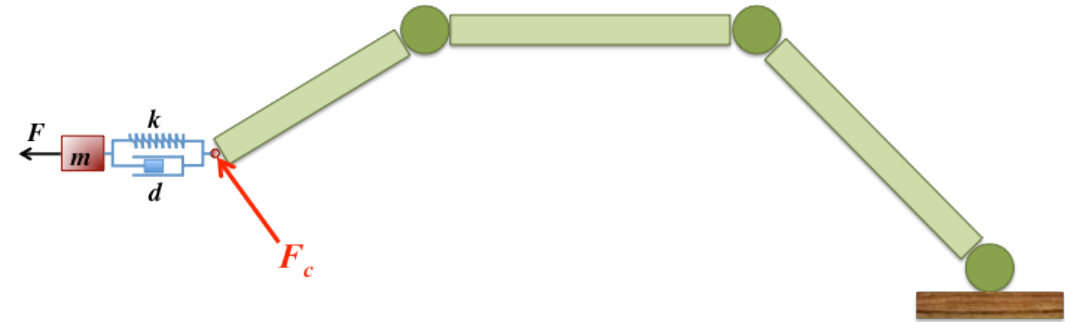
# Impedance-based control of interaction

Reaction to contact forces by generalized impedance —at **different** levels

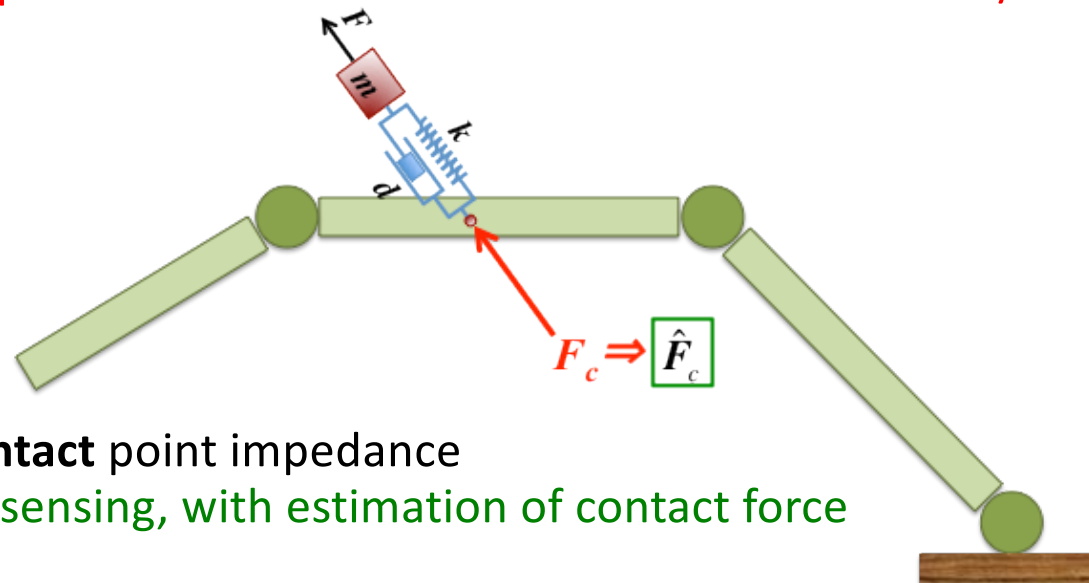
consider a fully rigid robot



**Joint impedance**  
needs joint torque sensors



**Cartesian impedance**  
needs F/T sensor



**Contact point impedance**  
without force/torque sensing, with estimation of contact force



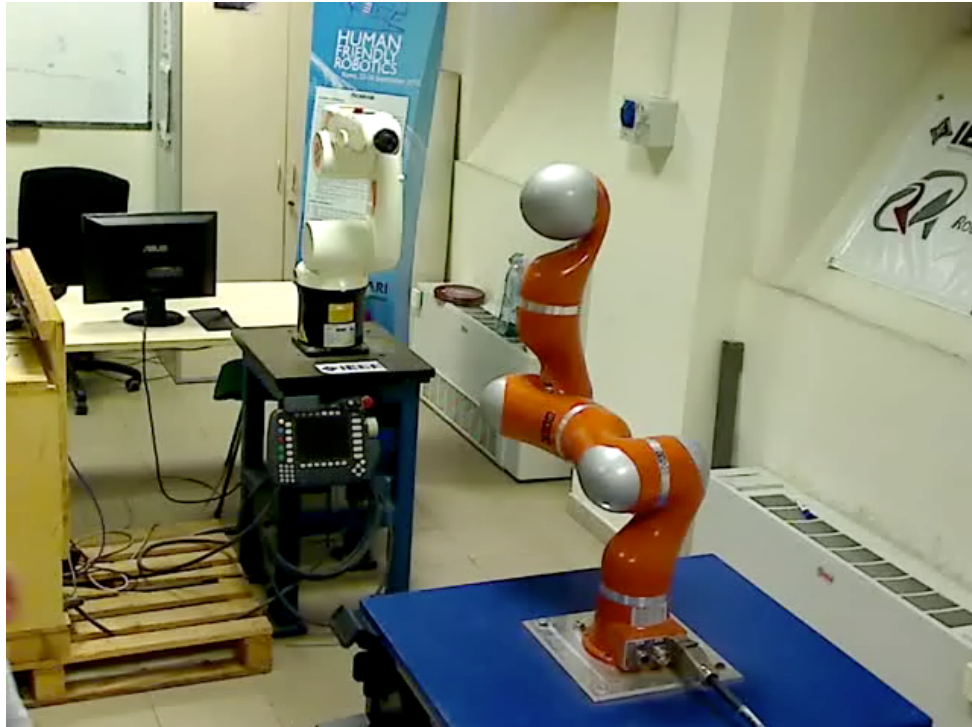
# Control of generalized impedance

HR collaboration at the contact level (ICRA 2015)

natural (unchanged) robot inertia **at the contact**

$$M_d = \left( J_c M^{-1} J_c^T \right)^{-1}$$

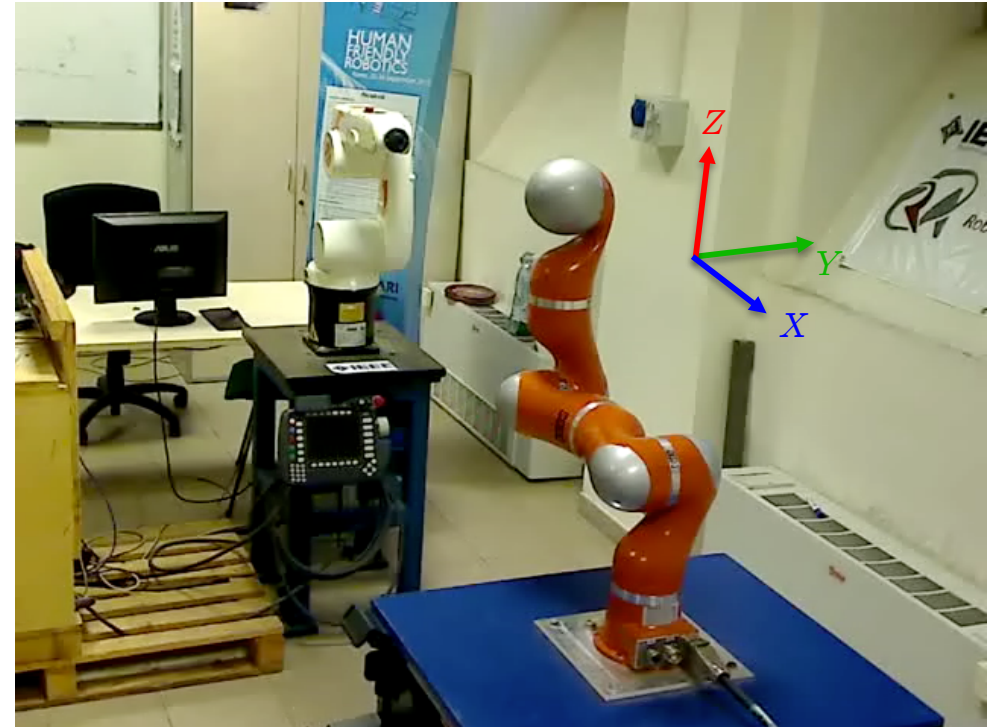
video



contact force **estimates** are used here  
**only** to detect and localize contact  
in order to start a collaboration phase

assigned robot inertia **at the contact**  
with different apparent masses along  $X$ ,  $Y$ ,  $Z$

video



contact force **estimates** used **explicitly** in  
control law to modify robot inertia at the contact  
( $M_{d,X} = 20$ ,  $M_{d,Y} = 3$ ,  $M_{d,Z} = 10$  [kg])



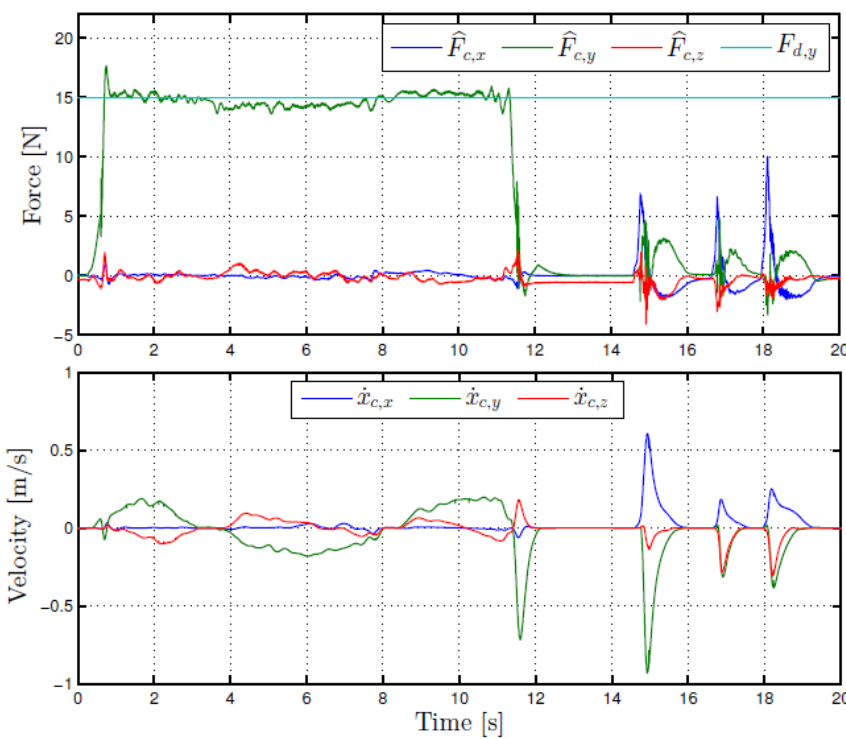
# Control of generalized contact force

## Direct force scheme

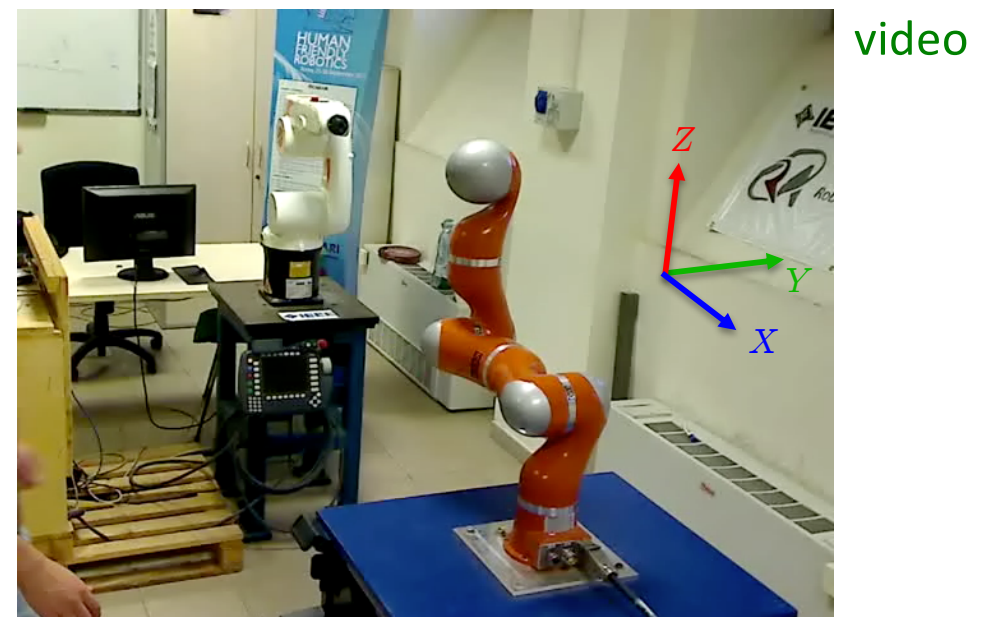
- explicit **regulation** of the **contact force** to a desired value, by imposing

$$M_d \ddot{x}_c + K_d \dot{x}_c = K_f (F_d - \hat{F}_c) = K_f e_f$$

- a force control law needs always a measure (here, an **estimate**) of contact force
- **task-compatibility:** human-robot contact direction vs. desired contact force vector



$$F_{d,x} = 0, \quad F_{d,y} = 15N, \quad F_{d,z} = 0$$



however, **drift effects** due to poor control design



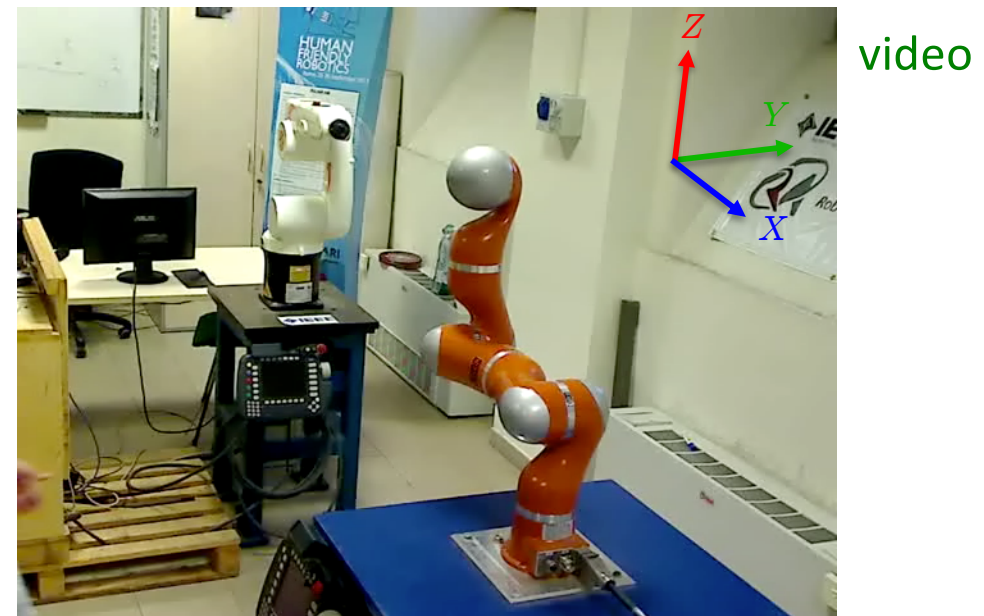
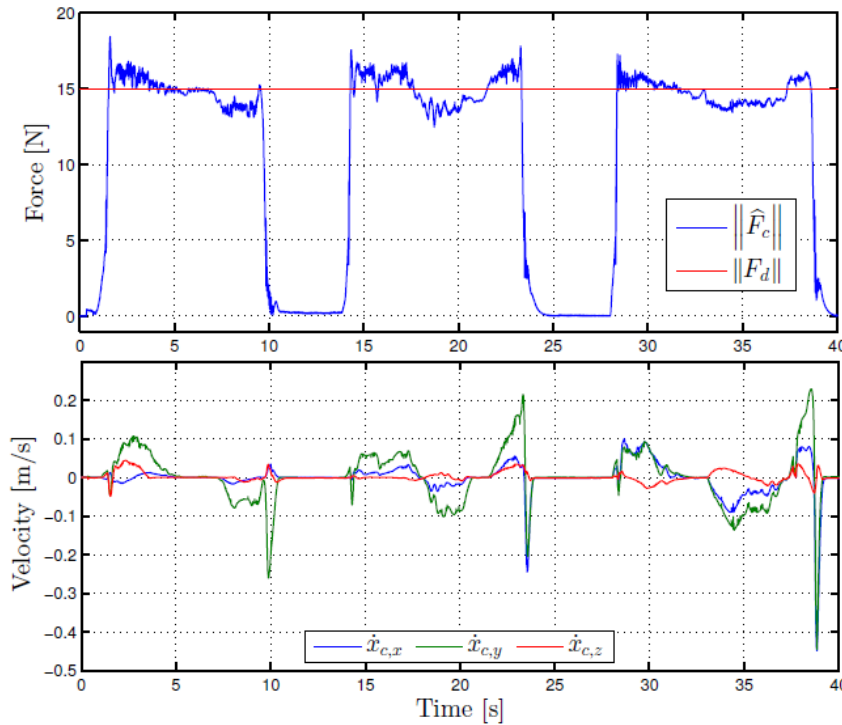
# Control of generalized contact force

Task-compatible force control scheme (ICRA 2015)

- only the **norm** of the desired contact force is controlled along the **instantaneous direction** of the **estimated contact force**

$$F_{d,x} = 15 \frac{\hat{F}_{c,x}}{\|\hat{F}_c\|}, \quad F_{d,y} = 15 \frac{\hat{F}_{c,y}}{\|\hat{F}_c\|}, \quad F_{d,z} = 15 \frac{\hat{F}_{c,z}}{\|\hat{F}_c\|} \Leftrightarrow \|F_d\| = 15 \text{ [N]}$$

- in static conditions, the force control law is able to regulate contact forces **exactly**



*task-compatible* control of contact force

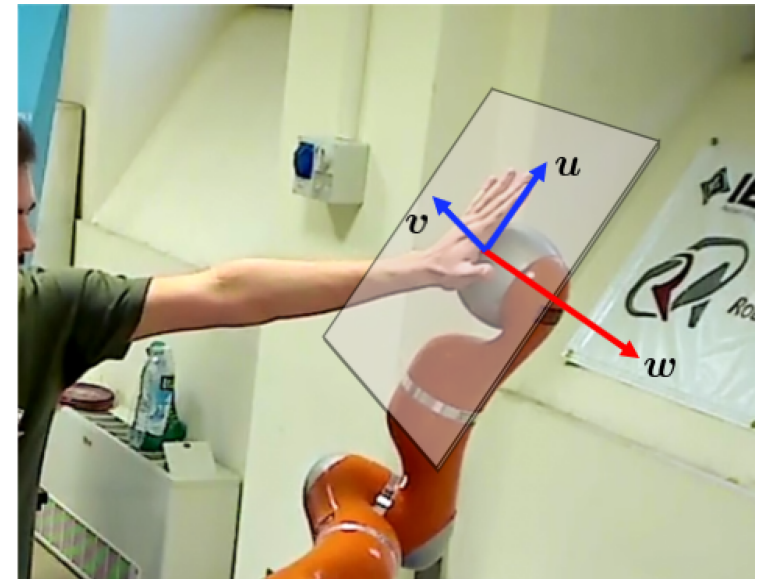


# Collaboration control

Hybrid force/velocity control scheme (ICRA 2016)

- it allows to control **both** contact force and motion in **two** mutually independent sub-spaces
- extends at the contact level a hybrid force/velocity control law, with the orientation of **contact task frame** being determined instantaneously
- task frame obtained by a rotation matrix  $R_t$  such that  $z_t$  is aligned with the **estimated** contact force

$$R_t = [ \begin{array}{ccc} u & v & w \end{array} ] = \left[ \begin{array}{ccc} u & v & \frac{\hat{F}_c}{\|\hat{F}_c\|}, \end{array} \right]$$



- after feedback linearization with  $\tau = Ma + n - J_c^T \hat{F}_c$ , the acceleration command is
$$a = J_c^\# M_d^{-1} (R_t a_c + M_d (\dot{R}_t {}^t \dot{x}_c - \dot{J}_c \dot{q})) + P_c \ddot{q}_0$$
- complete decoupling** between force control and velocity control can be achieved by choosing the new auxiliary control  $a_c$  input as

$$a_c = S_f^c \ddot{y}_f + S_\nu^c \dot{\nu}$$



# Collaboration control

## Hybrid force/velocity control scheme

- the force regulation task should be along the instantaneous direction of the applied external force while the motion control task lives in the orthogonal plane
- the **selection matrices** are chosen as

$$\mathbf{S}_f^c = \begin{bmatrix} 0 \\ 0 \\ 1 \end{bmatrix} \quad \mathbf{S}_\nu^c = \begin{bmatrix} 1 & 0 \\ 0 & 1 \\ 0 & 0 \end{bmatrix}$$

- regulation of the contact force to desired constant value  $F_d > 0$  is obtained choosing

$$\ddot{y}_f = k_f \left( F_d - \|\hat{\mathbf{F}}_c\| \right) - k_{df} \dot{y}_f$$

- control of the desired velocity can be achieved using

$$\dot{\boldsymbol{\nu}} = \dot{\boldsymbol{\nu}}_d + \mathbf{K}_d (\boldsymbol{\nu}_d - \boldsymbol{\nu}) + \mathbf{K}_i \int_0^t (\boldsymbol{\nu}_d - \boldsymbol{\nu}) ds,$$

- the final control acceleration input becomes

$$\begin{aligned} \mathbf{a} = \mathbf{J}_c^\# \mathbf{M}_d^{-1} \Big[ & \mathbf{R}_t \mathbf{S}_f^c (k_f e_f - k_{df} \dot{y}_f) + \mathbf{R}_t \mathbf{S}_\nu^c (\dot{\boldsymbol{\nu}}_d + \mathbf{K}_d \dot{\boldsymbol{\epsilon}}_\nu + \mathbf{K}_i \boldsymbol{\epsilon}_\nu) \\ & + \mathbf{M}_d \dot{\mathbf{R}}_t^c \dot{\mathbf{x}} - \mathbf{M}_d \dot{\mathbf{J}}_c \dot{\mathbf{q}} \Big] + \mathbf{P}_c \ddot{\mathbf{q}}_0, \end{aligned}$$

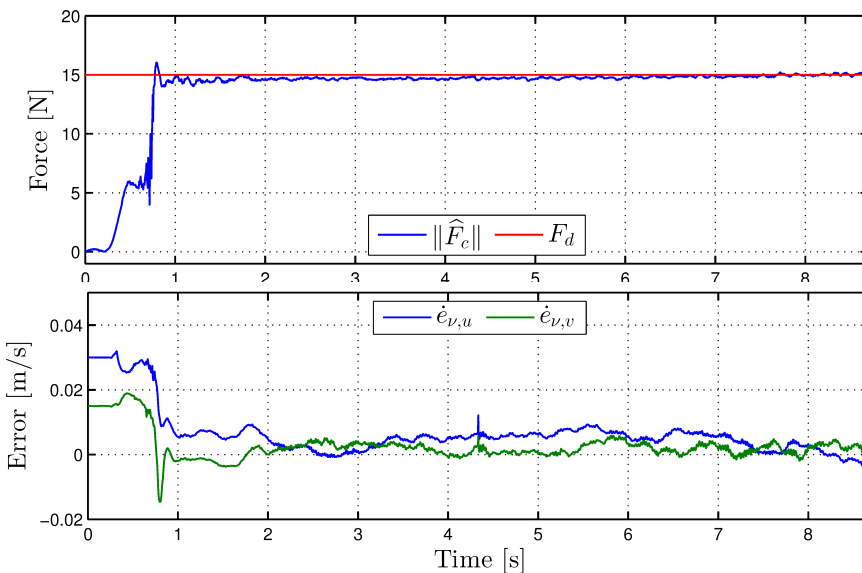


# Collaboration control

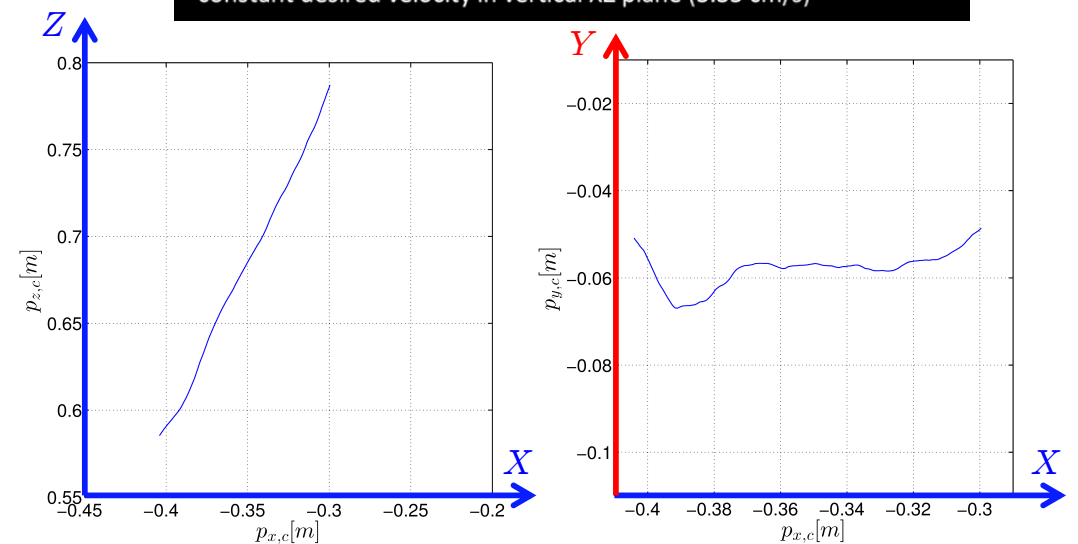
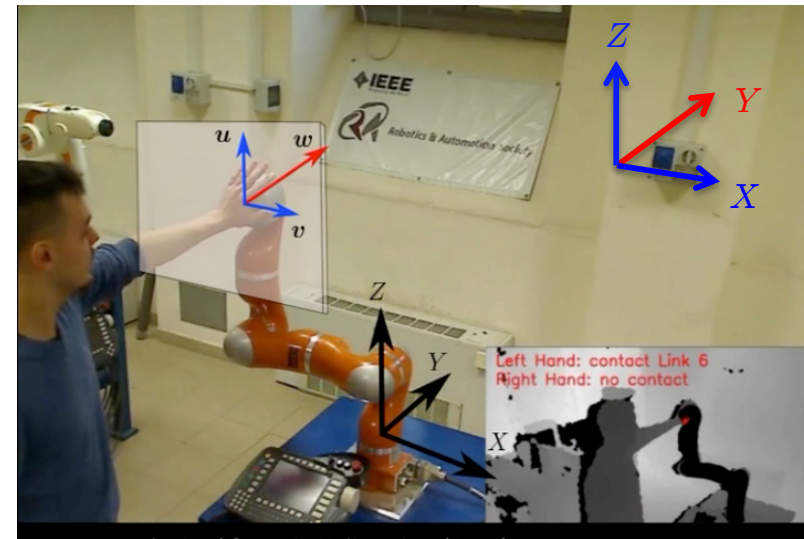
Hybrid force/velocity control at contact level (IROS 2016)

- desired contact force along  $Y$  direction regulated to  $F_d = 15[N]$
- constant desired velocity to perform a **line** in the **vertical  $XZ$  plane**

$$\nu_d = \begin{bmatrix} 0.015 \\ 0.03 \end{bmatrix} \quad \dot{\nu}_d = \begin{bmatrix} 0 \\ 0 \end{bmatrix}$$



<https://youtu.be/tlhEK5f00QU>



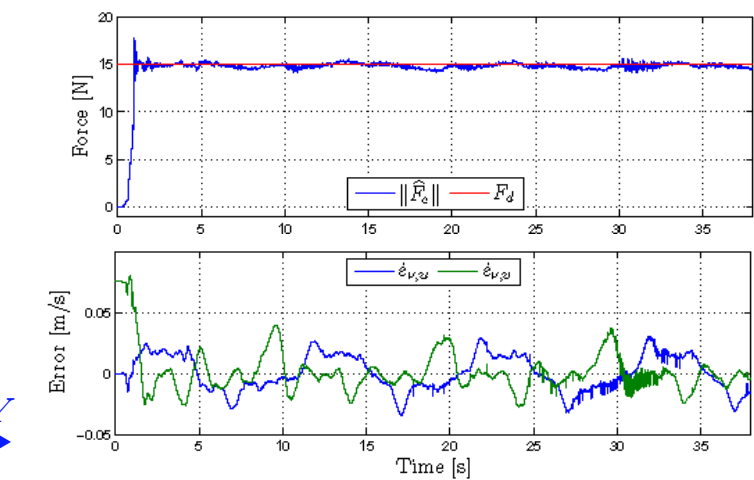
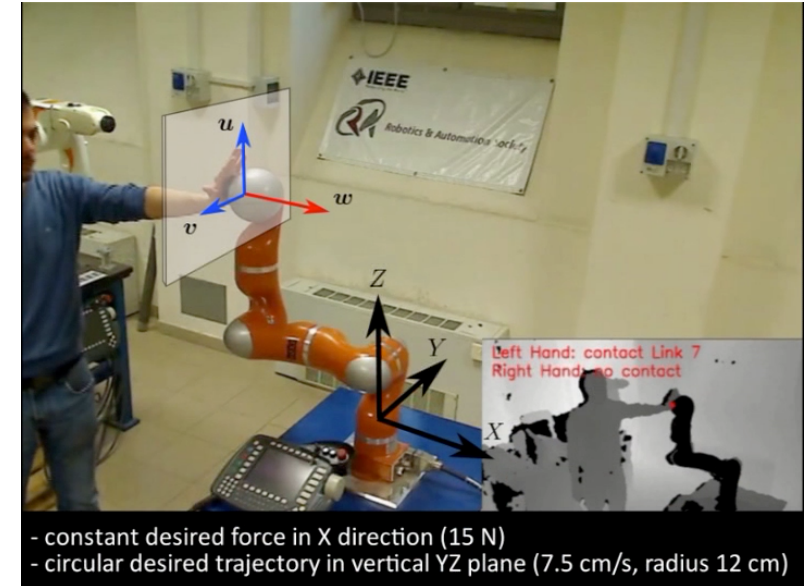
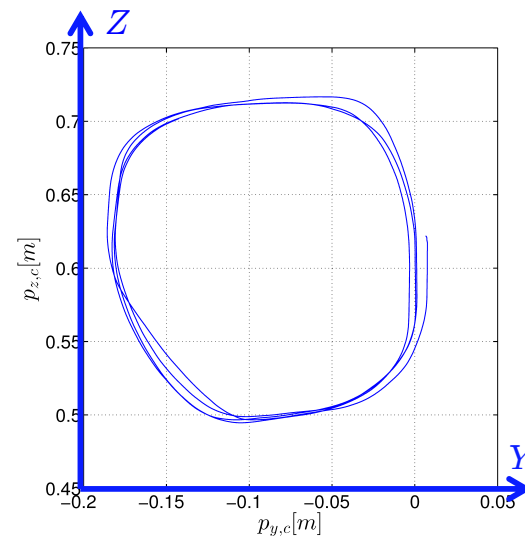
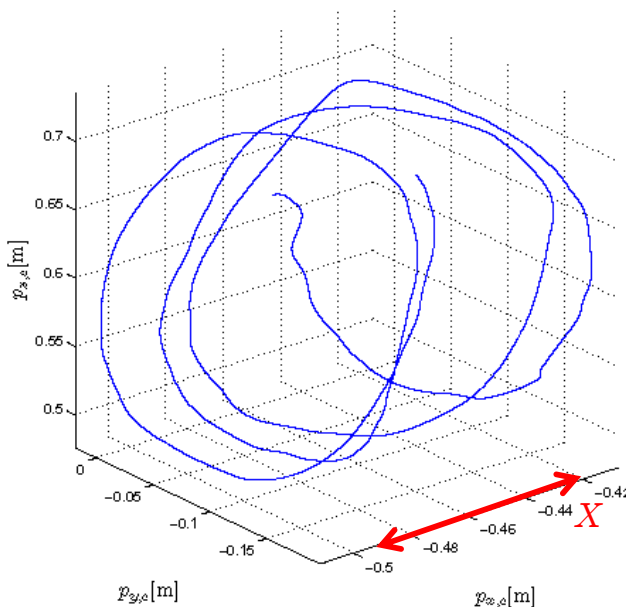


# Collaboration control

Hybrid force/velocity control at contact level (IROS 2016)

- desired contact force along the  $X$  direction regulated to  $F_d = 15[N]$
- desired velocity/acceleration to perform a **circle** in the vertical  $YZ$  plane

$$\nu_d = \begin{bmatrix} \omega\rho \sin \omega t \\ \omega\rho \cos \omega t \end{bmatrix} \quad \dot{\nu}_d = \begin{bmatrix} \omega^2\rho \cos \omega t \\ -\omega^2\rho \sin \omega t \end{bmatrix}$$

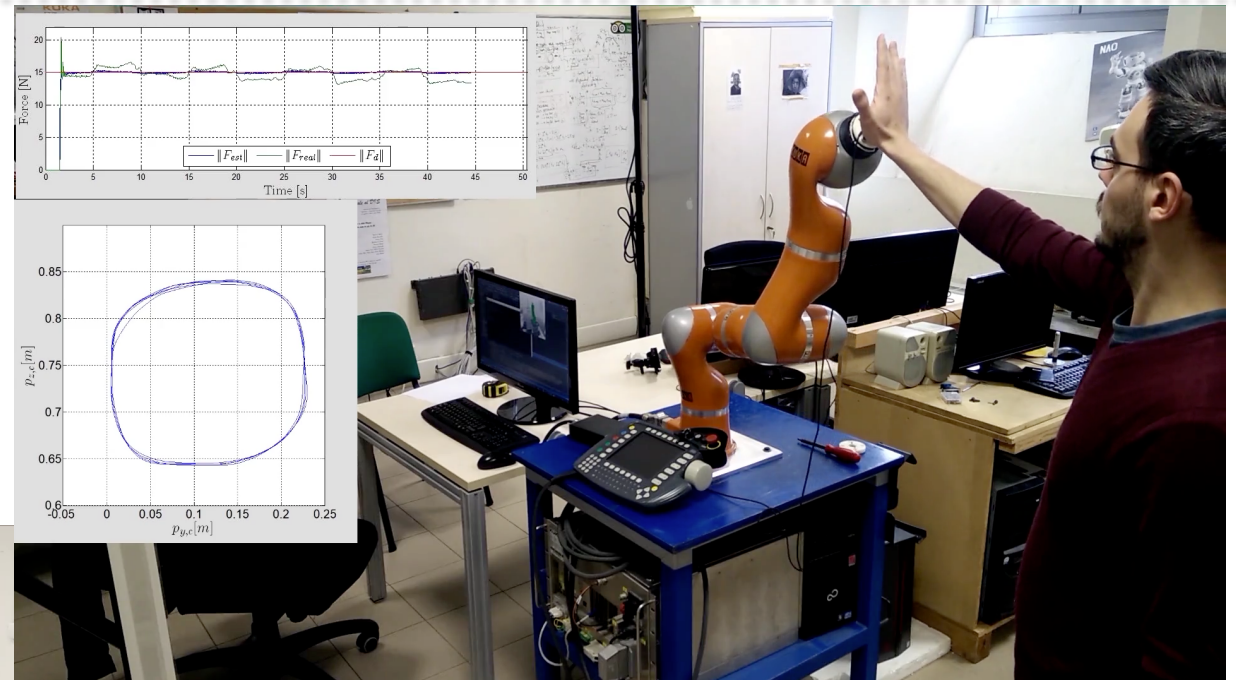




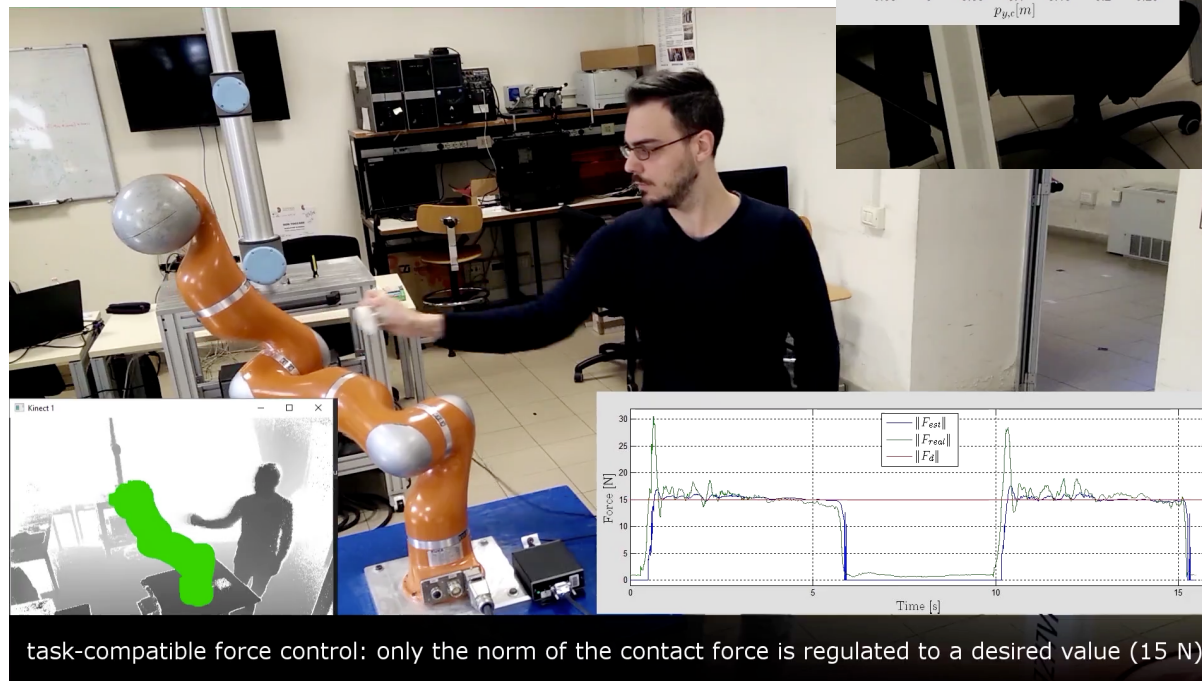
# Validation of collaboration control with a F/T sensor

Force and hybrid force/velocity control schemes at contact level (February 2019)

- desired contact force along the estimated contact direction regulated at 15 N
- ... and trajectory control with constant speed along a circle in the orthogonal plane



video



task-compatible force control: only the norm of the contact force is regulated to a desired value (15 N)

video



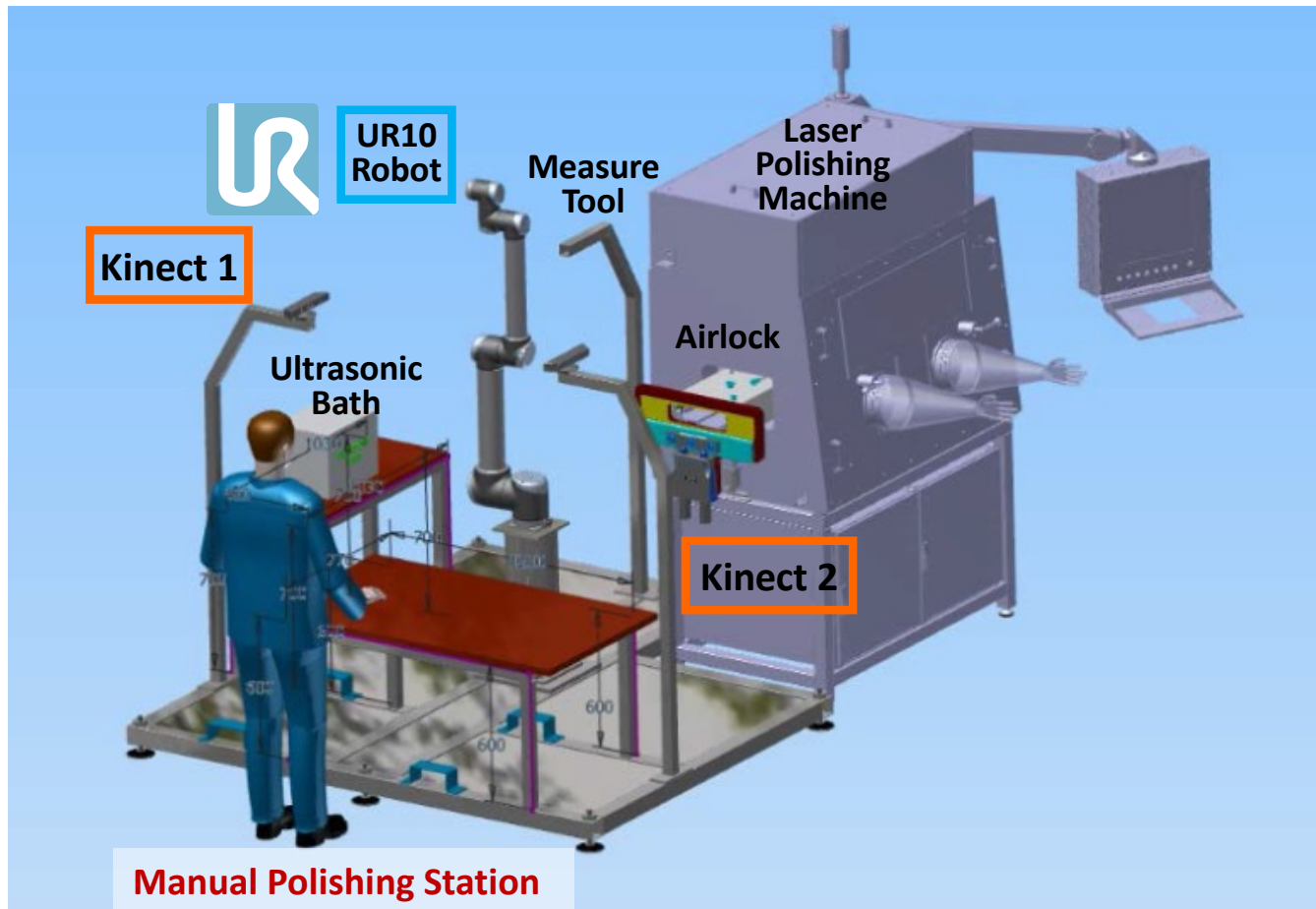
# SYMPLEXITY cell for laser polishing

Including a manual polishing station with **human-robot physical collaboration**



SYMPLEXITY

H2020 FoF EU project (2015-18)



Manual Polishing Station

Contact detection  
(model-based) for **safety**

3D workspace monitoring  
with 2 Kinects for  
**HR coexistence**

Use of F/T sensor  
and of residuals for  
**HR physical collaboration**

**Universal Robots UR10**

- lightweight design
- CE safety certified

**speed scaling/stop**  
from sensing HR distance  
(= **0** in physical collaboration)  
ISO/TS15066:2016



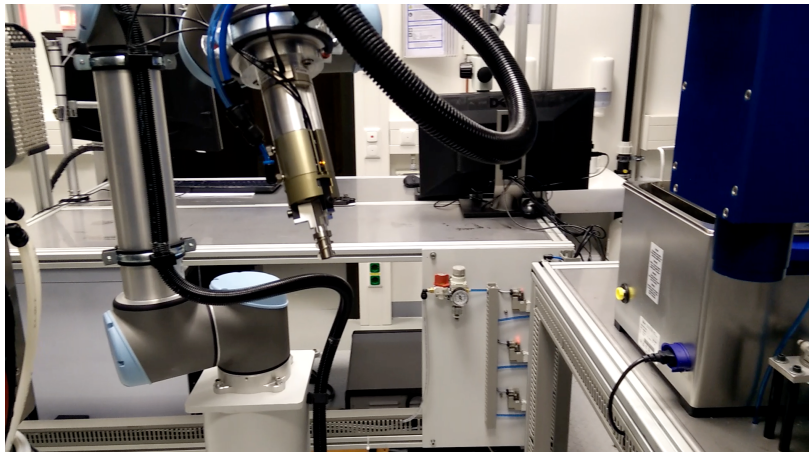
# Scenario for HRC in manual polishing

Preparing a metallic part for the final polishing by the laser machine

## UR10 robot operation with HR coexistence/collaboration

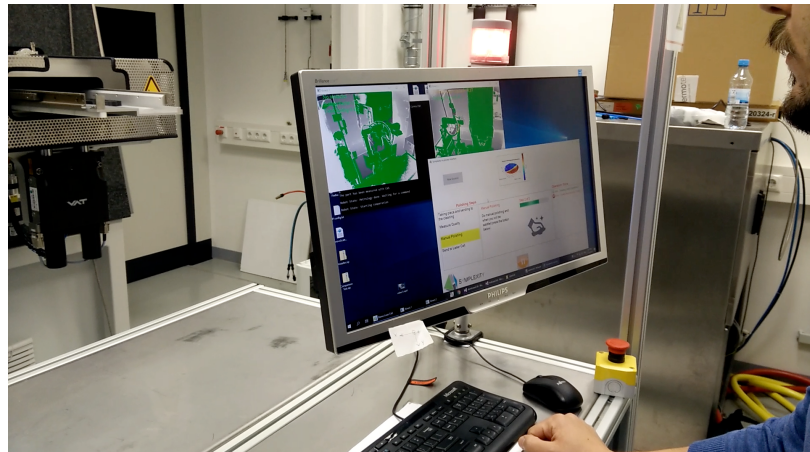


part to be  
polished



video

measuring Berlin Heart part with the CWS



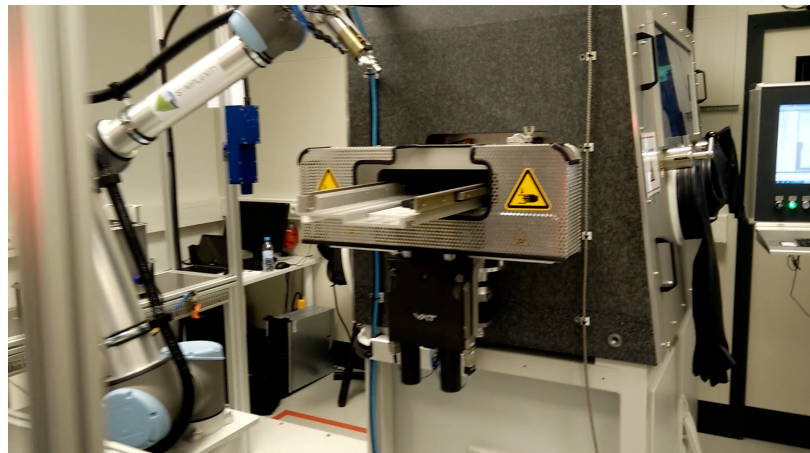
video

physical collaboration in contact



video

coexistence



video

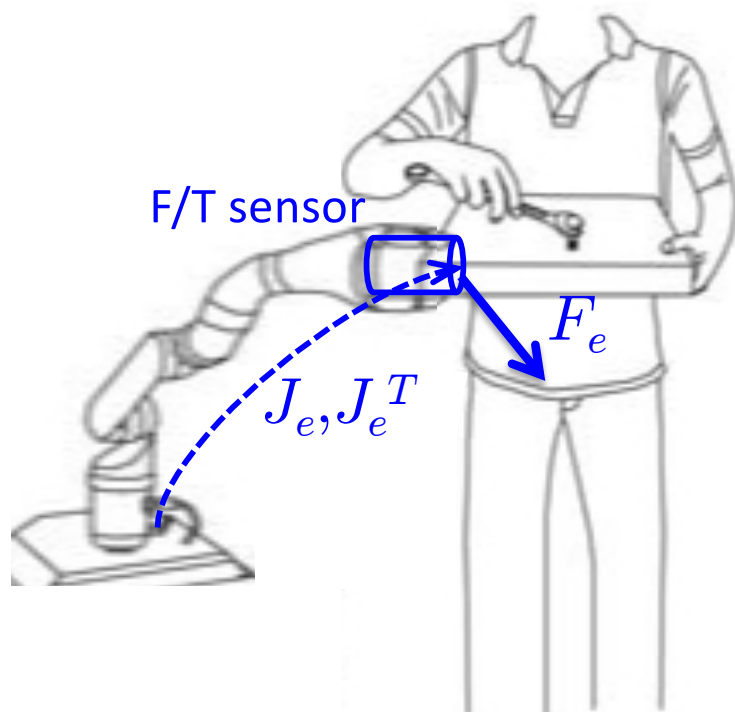
coordination with LP machine

CWS = Coherent Wave Scattering (laser measurement of surface quality)



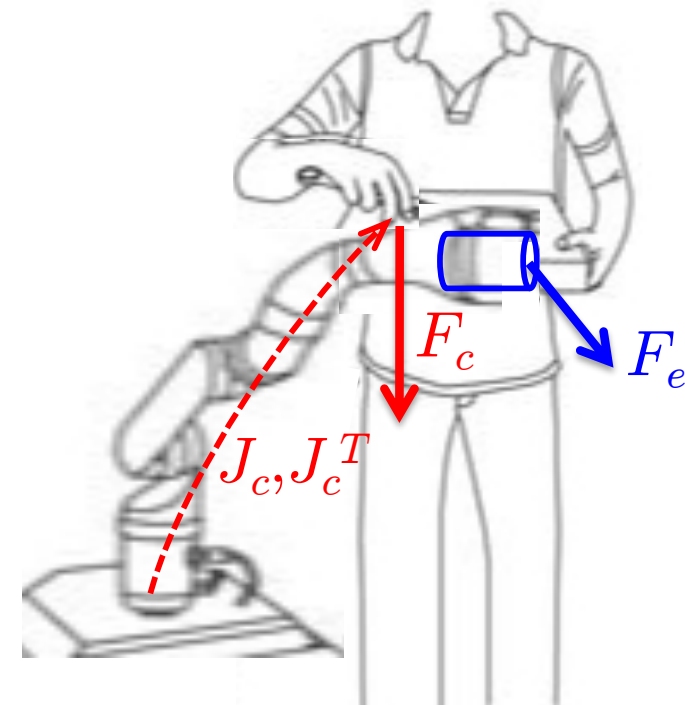
# Scenario for HRC in manual polishing

Distinguishing different contact forces



6D Force/Torque (F/T) sensor at wrist  
– manual polishing force is **measured**  
– end-effector Jacobian  $J_e$  is **known**

contact force at unknown location  
– **not** measurable by the F/T sensor  
– possibly applied by the human **while**  
manipulating the work piece held by robot  
– contact Jacobian  $J_c$  is **not** known





# Handling multiple contacts

Dynamic model and residual computation using also the F/T sensor

- robot **dynamic model** takes the form

$$M(q)\ddot{q} + \mathbf{S}(q, \dot{q})\dot{q} + g(q) = \boldsymbol{\tau} + J_e^T(q)\mathbf{F}_e + J_c^T(q)\mathbf{F}_c$$

- joint torques resulting from different contacts

(measured) at the end-effector level

at a generic point along the structure

$$\tau_e = J_e^T(q)F_e$$

$$\boldsymbol{\tau}_c = \boldsymbol{J}_c^T(\boldsymbol{q})\boldsymbol{F}_c$$

- monitor the robot generalized momentum  $p = M(q)\dot{q}$
  - (model-based) **residual vector** signal to detect and isolate the generic contacts

$$r(t) = K_i \left( p - \int_0^t \left( S^T(q, \dot{q})\dot{q} - g(q) + \tau + \textcolor{blue}{J_e^T(q)F_e} - r \right) ds \right)$$

$$K_i \rightarrow \infty \text{ (sufficiently large)} \quad \Rightarrow \quad r \simeq \tau_c$$



# Admittance control strategy during manual polishing

Human and robot are physically collaborating

- when there is no extra contact along the structure, **position and orientation** of the end-effector are both held **fixed** by a **stiff kinematic control law**

$$\dot{q} = J_e^\# K_e \begin{pmatrix} v_r \\ \omega_r \end{pmatrix} = J_e^\# K_e \begin{pmatrix} I & 0 \\ 0 & T(\phi) \end{pmatrix} \begin{pmatrix} p_d - p \\ \phi_d - \phi \end{pmatrix}$$

as large as possible ↑ constant values

- in this way, the control law counterbalances all forces/torques applied by the operator **during manual polishing**
- when the human intentionally pushes on the robot body, control of the end-effector **orientation is relaxed**

$$J_e(q) = \begin{pmatrix} J_p(q) \\ J_o(q) \end{pmatrix}$$

3x6 for UR10

residual-based  
admittance reaction  
to extra contacts

$$\dot{q} = J_p^\# K_p (p_d - p) + (I - J_p^\# J_p) K_r r$$

- human can reconfigure the arm, thus **reorient the work piece** held by the robot



# HRC phase with UR10 robot

Experimental verification in the lab (Mechatronics 2018)

[https://youtu.be/slwUiRT\\_IJQ](https://youtu.be/slwUiRT_IJQ)



Collaboration phase activated by hand waving (using a Kinect)

video

video

<https://youtu.be/bjZbmlAclYk>



## A Model-Based Residual Approach for Human-Robot Collaboration during Manual Polishing Operations

Claudio Gaz, Emanuele Magrini, Alessandro De Luca

Dipartimento di Ingegneria Informatica, Automatica  
e Gestionale, Sapienza Università di Roma

May 2017

no F/T sensor, switch to **UR FreeDrive** mode

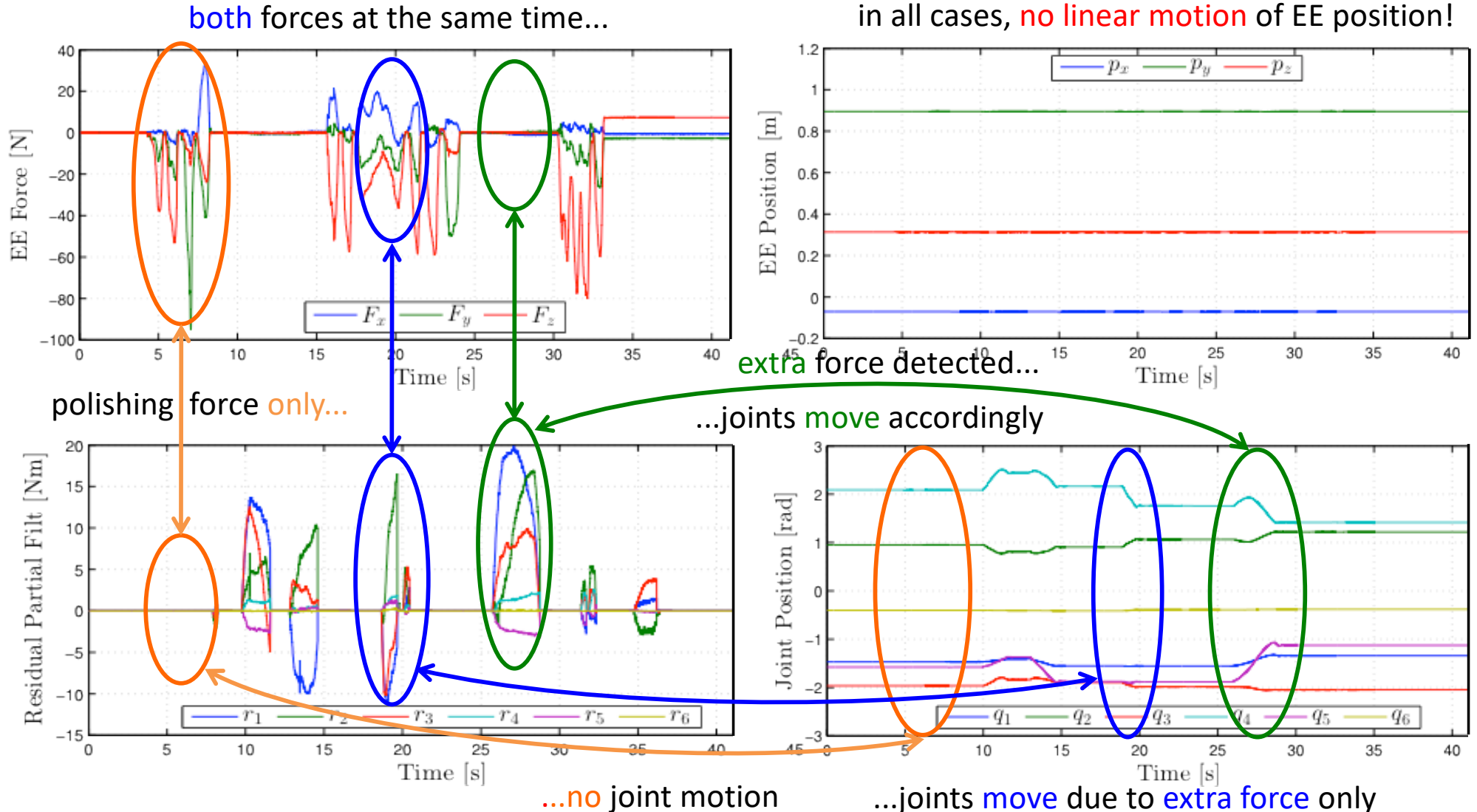
with F/T sensor, using our **residual** method

for a similar behavior with the KUKA LWR  
see <https://youtu.be/TZ6nPqLPDxI>



# HRC phase with UR10 robot

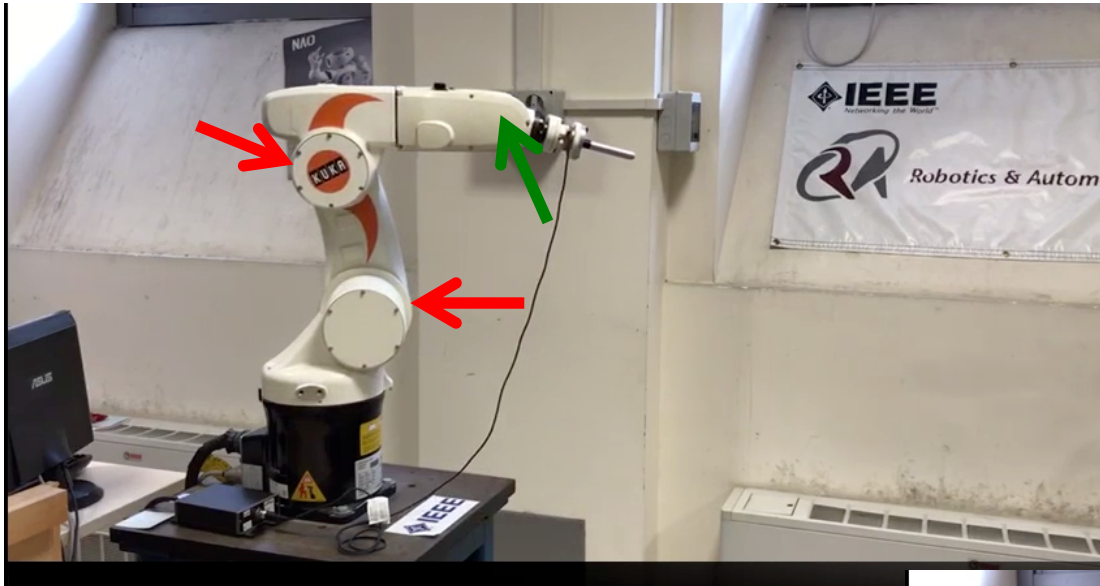
Experimental results (separating F/T measures from residuals)





# Combining motor currents and F/T sensor data

Enhanced flexible interaction by filtering, thresholding, merging signals (ICRA 2019)

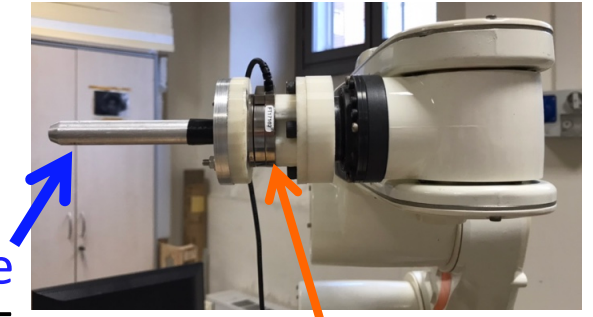


Robot in cyclic motion between four Cartesian positions

intentional contacts  
and/or collisions  
may occur anywhere

6-dof **KUKA KR5 Sixx** with  
**closed control** architecture  
and RSI interface at  $T_c = 12$  ms

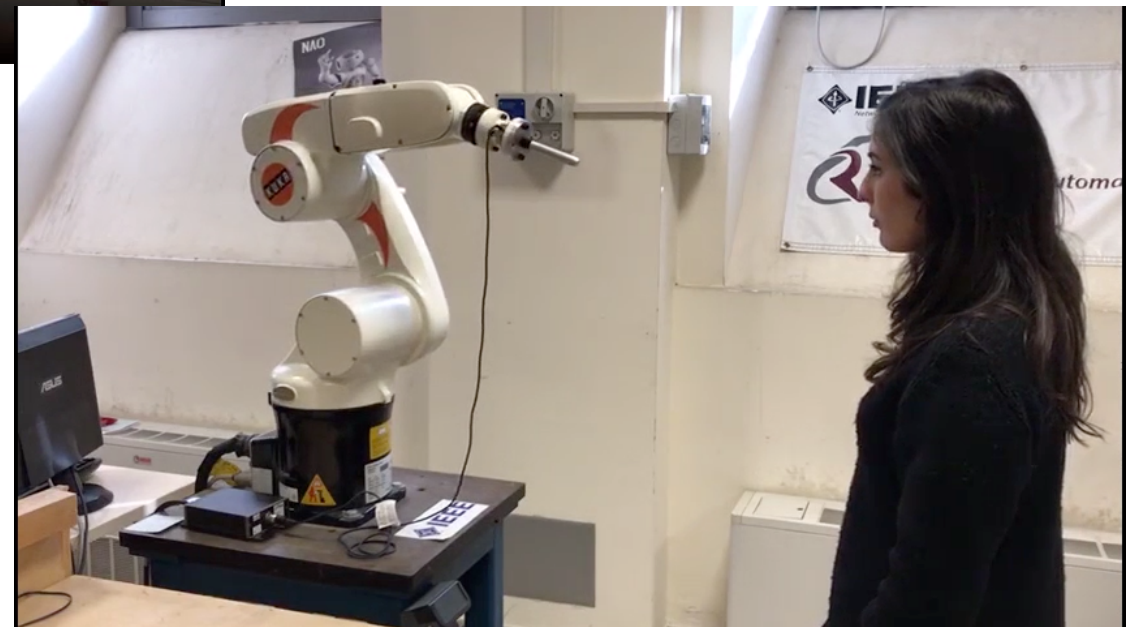
video



collaborative  
forces at E-E

ATI Mini45  
F/T sensor

video





## Our team at DIAG

Robotics Lab of the Sapienza University of Rome (back in 2014)



## Acknowledgements

@Sapienza – DIAG - Gabriele Buondonno, Lorenzo Ferrajoli, **Fabrizio Flacco<sup>†</sup>**,  
Claudio Gaz, Milad Geravand, Emanuele Magrini, Eleonora Mariotti, Raffaella Mattone

@DLR – Institute of Robotics and Mechatronics - Alin Albu-Schäffer, Sami Haddadin

@Stanford – Artificial Intelligence Lab - Oussama Khatib, Torsten Kröger



## References - 1

Download pdf for personal use at [www.diag.uniroma1.it/deluca/Publications](http://www.diag.uniroma1.it/deluca/Publications)

- A. De Luca and R. Mattone, "Sensorless robot collision detection and hybrid force/motion control," IEEE Int. Conf. on Robotics and Automation, pp. 999-1004, 2005.
- A. De Luca, A. Albu-Schäffer, S. Haddadin, and G. Hirzinger, "Collision detection and safe reaction with the DLR-III lightweight manipulator arm," IEEE/RSJ Int. Conf. on Intelligent Robots and Systems, pp. 1623-1630, 2006.
- S. Haddadin, A. Albu-Schäffer, A. De Luca, and G. Hirzinger, "Collision detection and reaction: A contribution to safe physical human-robot interaction," IEEE/RSJ Int. Conf. on Intelligent Robots and Systems, pp. 3356-3363, 2008 (**IROS 2008 Best Application Paper Award**).
- A. De Luca and L. Ferrajoli, "Exploiting robot redundancy in collision detection and reaction," IEEE/RSJ Int. Conf. on Intelligent Robots and Systems, pp. 3299-3305, 2008.
- A. De Santis, B. Siciliano, A. De Luca, A. Bicchi, "An atlas of physical human-robot interaction," Mechanism and Machine Theory, vol. 43, no. 3, pp. 253–270, 2008 (**2017 MMT Award for Excellence**).
- A. De Luca and L. Ferrajoli, "A modified Newton-Euler method for dynamic computations in robot fault detection and control," IEEE Int. Conf. on Robotics and Automation, pp. 3359-3364, 2009.
- F. Flacco, A. De Luca, "Multiple depth/presence sensors: Integration and optimal placement for human/robot coexistence," IEEE Int. Conf. on Robotics and Automation, pp. 3916-3923, 2010.
- F. Flacco, T. Kröger, A. De Luca, and O. Khatib, "A depth space approach to human-robot collision avoidance," IEEE Int. Conf. on Robotics and Automation, pp. 338-345, 2012.
- A. De Luca and F. Flacco, "Integrated control for pHRI: Collision avoidance, detection, reaction and collaboration," 4th IEEE RAS Int. Conf. on Biomedical Robotics and Biomechatronics, pp. 288-295, 2012 (**BioRob 2012 Best Paper Award**).
- M. Geravand, F. Flacco, and A. De Luca, "Human-robot physical interaction and collaboration using an industrial robot with a closed control architecture," IEEE Int. Conf. on Robotics and Automation, pp. 3985-3992, 2013.
- E. Magrini, F. Flacco, and A. De Luca, "Estimation of contact force using a virtual force sensor," IEEE/RSJ Int. Conf. on Intelligent Robots and System, pp. 2126-2133, 2014.
- F. Flacco, T. Kröger, A. De Luca, and O. Khatib, "A depth space approach for evaluating distance to objects —with application to human-robot collision avoidance," J. of Intelligent & Robotic Systems, vol. 80 S.1, pp. 7-22, 2015.



## References - 2

Download pdf for personal use at [www.diag.uniroma1.it/deluca/Publications](http://www.diag.uniroma1.it/deluca/Publications)

- E. Magrini, F. Flacco, and A. De Luca, "Control of generalized contact motion and force in physical human-robot interaction," IEEE Int. Conf. on Robotics and Automation, pp. 2298-2304, 2015 (ICRA 2015 Best Conference Paper Award Finalist).
- G. Buondonno and A. De Luca, "Combining real and virtual sensors for measuring interaction forces and moments acting on a robot," IEEE/RSJ Int. Conf. on Intelligent Robots and Systems, pp. 794-800, 2016.
- E. Magrini and A. De Luca, "Hybrid force/velocity control for physical human-robot collaboration tasks," IEEE/RSJ Int. Conf. on Intelligent Robots and Systems, pp. 857-863, 2016.
- F. Flacco and A. De Luca, "Real-time computation of distance to dynamic obstacles with multiple depth sensors," IEEE Robotics and Automation Lett., vol. 2, no. 1, pp. 56-63, 2017.
- M. Khatib, K. Al Khudir, A. De Luca, "Visual coordination task for human-robot collaboration," IEEE/RSJ Int. Conf. on Intelligent Robots and Systems, pp. 3762-3768, 2017.
- E. Magrini, A. De Luca, "Human-robot coexistence and contact handling with redundant robots," IEEE/RSJ Int. Conf. on Intelligent Robots and Systems, pp. 4611-4617, 2017.
- S. Haddadin, A. De Luca, and A. Albu-Schäffer, "Robot collisions: A survey on detection, isolation, and identification," IEEE Trans. on Robotics, vol. 33, no. 6, pp. 1292-1312, 2017.
- C. Gaz, A. De Luca, "Payload estimation based on identified coefficients of robot dynamics --with an application to collision detection," IEEE/RSJ Int. Conf. on Intelligent Robots and Systems, pp. 3033-3040, 2017.
- C. Gaz, E. Magrini, A. De Luca, "A model-based residual approach for human-robot collaboration during manual polishing operations," Mechatronics, vol. 55, pp. 234-247, 2018.
- E. Mariotti, E. Magrini, A. De Luca, "Admittance control for human-robot interaction using an industrial robot equipped with a F/T sensor," IEEE Int. Conf. on Robotics and Automation, pp. 6130-6136, 2019.
- E. Magrini, F. Ferraguti, A.J. Ronga, F. Pini, A. De Luca, F. Leali, "Human-robot coexistence and interaction in open industrial cells," Robotics and Computer-Integrated Manufacturing, vol. 61, 101846, 2020.
- **Videos:** YouTube channel [RoboticsLabSapienza](https://www.youtube.com/user/RoboticsLabSapienza). Playlist: [Physical human-robot interaction](https://www.youtube.com/playlist?list=PLD9BzXWVjyfCwvLcOOGdXGKQHgkPmUo)